

Holographic mean field theory and Kondo lattice

Young-Kwon Han, Debabrata Ghorai, Taewon Yuk, Sang-Jin Sin

*Department of Physics, Hanyang University,
Seoul, 04763, South Korea*

E-mail: youngkwonhan346@gmail.com, dghorai123@gmail.com,
tae1yuk@gmail.com, sangjin.sin@gmail.com

ABSTRACT: We first study a non-relativistic field theory model for the Kondo lattice by introducing the Kondo condensation, whose main effect is the hybridization of the flat band of the localized electron with dispersive one of the itinerant electron. The problem here is that the resulting Kondo condensation arises only in strong coupling where the validity of the mean field theory is questionable. Therefore, we build a holographic mean field theory of the Kondo lattice with strong coupling by identifying the effect of the lattice with the fermion's spectral shape due to the coupling with the order parameter representing the symmetry breaking. For the flat band spectrum we use the mixed quantization, and for the dispersive spectrum we introduce the second fermion in standard quantization. The coupling of the two fermions with the scalar order representing the Kondo condensation provides the hybridization of the two spectrum, reproducing the main feature of the Kondo lattice together with the fuzzy character of the spectrum of the strongly coupled system.

KEYWORDS: Kondo Condensation, Holographic Mean Field Theory, Quantum Phase Transition

Contents

1	Introduction	1
2	Non-relativistic mean field model for the Kondo condensation	4
2.1	Setup	4
2.2	Energy-momentum dispersion	5
2.3	Formation of the Kondo condensation	6
3	Holographic Kondo lattice model	8
3.1	Setup	8
3.2	Background fields	9
3.3	Probe spinor fields	11
3.3.1	Equations of motion of the probe spinor fields	11
3.3.2	Probe spinor fields near the boundary	12
3.4	Spectral function and density of states	13
4	Conclusion	14
A	Thermodynamic potential of the non-relativistic mean field model	15
B	Numerical calculation of the non-relativistic mean field model	17
C	Details of the holographic Kondo lattice model	18
C.1	Probe spinor fields in the bulk	18
C.2	Probe spinor fields near the horizon	20
C.3	From standard-standard to standard-mixed quantization	21
D	Trial holographic models for the Kondo lattice	22
D.1	With $g_1 \Phi_{\text{ps}} \cdot i\mathbb{I}_4$ rather than $g_1 \Phi_{\text{ps}} \cdot \Gamma^5$	22
D.2	Without $g_2 \Phi_{\text{s}} \cdot i\mathbb{I}_4$	24

1 Introduction

The Kondo effect describes the scattering of conduction electrons in a metal due to localized magnetic impurities, leading to the minimum of the resistance as a function of temperature. Since its discovery in 1930 [1], it has been one of the leading motivations in developing modern quantum field theory as well as in the physics of strongly correlated condensed matter.

In 1961, P. W. Anderson introduced the exchange interaction between the localized electron in the d -orbital and itinerant electrons in the s -orbital to explain the presence

of the localized magnetic moment in metals [2]. In 1964, based on the coupling between the spin impurity and itinerant electron introduced in refs. [3–7], J. Kondo explained the resistance minimum [8] using the third-order perturbative field theory of another s - d exchange model. His result is summarized as a logarithmic contribution, $\ln T_c/T$, to the resistivity. The Kondo temperature, T_c , is the limit below which his result is not valid, and the divergence problem in the $T \rightarrow 0$ limit was resolved by K. Wilson in the 1970s by inventing the modern concept of renormalization group [9]. In the late 1960s, J. R. Schrieffer and his collaborators [10, 11] showed that the Kondo model is a low-energy effective model of the Anderson model using a canonical transformation, which is now called Schrieffer-Wolff transformation, that projects out the high-energy degrees of freedom. From the modern point of view, because the interaction is marginally relevant, the Kondo model lies in the strong coupling regime of the Anderson impurity model, so the Kondo problem is essentially the physics of a strongly coupled system. A great deal of research on Kondo systems followed afterward, using the large- N approach, renormalization group, and conformal field theory [11–25], and the Kondo physics has been the testing ground of new ideas for the non-perturbative or exact calculational method.

When the density of impurities is low, we do not need to consider the impurity-impurity correlation, and we may consider one impurity problem. For higher density impurities, the problem can be classified into random impurities and impurity lattice. For the latter, the Kondo effect likely explains the formation of heavy fermions and Kondo insulators. The main expected characteristic of the Kondo lattice [14, 26] is the enlarged Fermi surface of heavy fermions formed by the hybridization of itinerant electrons and localized magnetic impurities forming a regular lattice structure. For the former, the concept of the Kondo condensation, the condensation of the pair of the itinerant electrons and the magnetic impurities in the Kondo lattice, i.e., a magnetic version of the Bardeen-Cooper-Schrieffer pair condensation was suggested, and it was experimentally observed [27]. Independently, mean field studies on the condensation of the pair of heavy and light fermions have been done to study the Kondo lattice [28–35] using a continuum relativistic field theory based on the Nambu-Jona-Lasinio model [36, 37].

In this paper, we begin by analyzing a non-relativistic field theory model for the Kondo lattice to simplify the relativistic model [28–35] and to consider higher-order corrections effectively. We show that the Fierz identity and the mean field approximation relate our model to the continuum version of the Anderson model without the Schrieffer-Wolff transformation. We also find that if only the vector-type s - d interaction term exists in our model, then it is unstable. Hence, we add a scalar-type s - d coupling to stabilize the system. We introduce both scalar and vector types of the Kondo condensation and show that the Kondo condensation forms when the temperature is low and the s - d mixing is strong. The type of the Kondo condensation is determined by the relation between vector- and scalar-type coupling constants. We focus on the case where only the scalar-type Kondo condensation forms so that our model can be reduced to a lattice version of the Anderson model. The phase transition in this model is a first-order quantum phase transition.

As we mentioned before, the Kondo condensation forms only if the heavy-light coupling is strong, for which case the mean field theory is not supposed to work. The subtlety

in the usual large- N approaches to justify the mean field approximation is that there is no such number in real materials. To resolve these problems, we try to describe the Kondo condensation in the Kondo lattice using the holographic framework [38–45], which is supposed to handle strong correlations.

In fact, various holographic studies about single-impurity systems have already been performed before. One approach is in the top-down manner by considering the single impurity described by a $D(8-p)$ -brane, where p is the spatial dimension of the dual gauge theory [46–56]. Another one is a bottom-up approach considering the Chern-Simons gauge field in the Bañados-Teitelboim-Zanelli black hole background and the Yang-Mills gauge field in a localized AdS_2 subspace, where the information of the single impurity is encoded in the flux of the Yang-Mills field [57–65]. Some similarities between the fractionalized Fermi liquid phase of a lattice-impurity system and the holographic metals were also pointed out [66, 67]. The ref. [27] suggested a holographic Kondo model of dense random impurities described by the scalar-type Kondo condensation.

Yet, there has not been any holographic Kondo lattice model that gives the fermionic spectrum even within the simplest bottom-up approach. In fact, the holographic theory is a continuum field theory describing a low-energy effective theory, and introducing lattice eliminates the small spacetime structure, destroying the continuum structure. This is a challenge.

Recently, we developed the holographic mean field theory [68, 69], where the fermion bilinear is coupled to order parameter fields of various tensor types. The non-zero order parameter of a particular tensor type corresponds to a specific rotational symmetry breaking. With various symmetry breaking types, the fermion spectral functions produce features like separated Dirac cones, nodal lines, flat bands as well as gaps of s- p- and d-wave types. In fact, these exhaust important features that can be produced by lattices. We interpret this as the realization of the lattice in the continuum field theory with symmetry breaking. In other words, the role of the lattice in the low energy is nothing but a particular type of rotational symmetry breaking.

Extending this idea, we define a holographic Kondo lattice as the holographic mean field theory which produces the spectrum that is expected in the Kondo lattice, that is, a band structure that is a hybridization of a flat band with a hyperbolic one. The holographic flat band has already been realized in ref. [70] by the mixed quantization, and it was interpreted [71] as the consequence of cancelation between the two components, which is precisely the mechanism for producing the flat bands by forming the compact localized orbits in lattice models. The rest of the idea is to introduce another holographic fermion in standard quantization [68, 72–81] and give interaction between the two flavors to hybridize the spectrum.

In summary, after getting intuition from our non-relativistic mean field theory, we construct an effective model for the Kondo lattice in the holographic framework of spinors using the standard-mixed quantization. Finally, by calculating the fermionic spectral function and the density of states following the standard lore, we show that our proposed holographic Kondo lattice model indeed produces the main features of the Kondo condensation in the Kondo lattice system including the extended Fermi volume as well as the

large fermion mass.

In section 2, we study the mean field theory in the non-relativistic framework. In section 3, we construct a holographic mean field theory for the Kondo lattice and calculate the spectral functions. We summarize and discuss in section 4. There are four appendices describing the mathematical details, which are omitted in the main text.

2 Non-relativistic mean field model for the Kondo condensation

2.1 Setup

Based on refs. [4–8, 28–37], we construct a non-relativistic model for the Kondo lattice in continuum limit as follows:

$$\begin{aligned} \mathcal{L} = & \psi^\dagger \left(i \frac{\partial}{\partial t} + \frac{\nabla^2}{2m} + \mu \right) \psi + \chi^\dagger \left(i \frac{\partial}{\partial t} - \lambda \right) \chi \\ & + \frac{g_l}{2} (\psi^\dagger \psi)^2 - g_s (\psi^\dagger \psi) (\chi^\dagger \chi) - g_v (\psi^\dagger \vec{\sigma} \psi) \cdot (\chi^\dagger \vec{\sigma} \chi). \end{aligned} \quad (2.1)$$

$\psi \equiv (\psi_\uparrow, \psi_\downarrow)^T$ and $\chi \equiv (\chi_\uparrow, \chi_\downarrow)^T$ describe the light and heavy fermions, respectively. m is the mass of the light fermion. μ is the chemical potential for the light fermion. λ is the energy level of the heavy fermion without hybridization. $\vec{\sigma} = (\sigma_1, \sigma_2, \sigma_3)$ are the Pauli matrices. g_l is the light-light coupling constant. g_s and g_v are the scalar- and vector-type heavy-light coupling constants, respectively. Using the Fierz identity, we can write the Lagrangian as

$$\begin{aligned} \mathcal{L} = & \psi^\dagger \left(i \frac{\partial}{\partial t} + \frac{\nabla^2}{2m} + \mu \right) \psi + \chi^\dagger \left(i \frac{\partial}{\partial t} - \lambda \right) \chi \\ & + \frac{g_l}{2} (\psi^\dagger \psi)^2 + g'_s (\psi^\dagger \chi) (\chi^\dagger \psi) + g'_v (\psi^\dagger \vec{\sigma} \chi) \cdot (\chi^\dagger \vec{\sigma} \psi), \end{aligned} \quad (2.2)$$

where

$$g'_s := \frac{g_s + 3g_v}{2}, \quad g'_v := \frac{g_s - g_v}{2}. \quad (2.3)$$

The Hubbard-Stratonovich transformation with M and the Kondo condensation $\Delta \sim \langle \psi^\dagger \chi \rangle$,

$$\frac{g_l}{2} (\psi^\dagger \psi)^2 \rightarrow -\frac{M^2}{2g_l} - M(\psi^\dagger \psi), \quad (2.4)$$

$$g'_s (\psi^\dagger \chi) (\chi^\dagger \psi) \rightarrow -\frac{|\Delta_s|^2}{g'_s} + \Delta_s (\chi^\dagger \psi) + (\psi^\dagger \chi) \Delta_s^*, \quad (2.5)$$

$$g'_v (\psi^\dagger \vec{\sigma} \chi) \cdot (\chi^\dagger \vec{\sigma} \psi) \rightarrow -\frac{|\Delta_v|^2}{g'_v} + \vec{\Delta}_v \cdot (\chi^\dagger \vec{\sigma} \psi) + (\psi^\dagger \vec{\sigma} \chi) \cdot \vec{\Delta}_v^*, \quad (2.6)$$

gives the following mean field Lagrangian

$$\mathcal{L}_{\text{MF}} = \Psi^\dagger D \Psi - U, \quad (2.7)$$

where

$$\Psi^\dagger := \begin{pmatrix} \psi^\dagger & \chi^\dagger \end{pmatrix}, \quad \Psi := \begin{pmatrix} \psi \\ \chi \end{pmatrix}, \quad (2.8)$$

$$D := \begin{pmatrix} i\frac{\partial}{\partial t} + \frac{\nabla^2}{2m} + \mu - M & \Delta_s^* + \vec{\sigma} \cdot \vec{\Delta}_v^* \\ \Delta_s + \vec{\sigma} \cdot \vec{\Delta}_v & i\frac{\partial}{\partial t} - \lambda \end{pmatrix}, \quad (2.9)$$

$$U := \frac{M^2}{2g_l} + \frac{|\Delta_s|^2}{g'_s} + \frac{|\vec{\Delta}_v|^2}{g'_v}. \quad (2.10)$$

The thermodynamic potential is given by (see appendix A and ref. [82])

$$\begin{aligned} \Omega &= U + \frac{1}{V} \sum_{|\vec{p}| < \Lambda} \sum_{i=1}^4 \left\{ -\frac{1}{2} |\omega_i(\vec{p})| - \frac{1}{\beta} \ln \left[1 + e^{-\beta |\omega_i(\vec{p})|} \right] \right\} \\ &= U - \frac{1}{4\pi^2} \int_0^\Lambda dp p^2 \sum_{i=1}^4 |\omega_i(p)| - \frac{1}{2\pi^2 \beta} \int_0^\Lambda dp p^2 \sum_{i=1}^4 \ln \left[1 + e^{-\beta |\omega_i(p)|} \right], \end{aligned} \quad (2.11)$$

where $T \equiv 1/\beta$ is the temperature, Λ is the momentum cutoff, and $\omega_i(\vec{p})$ is the energy-momentum dispersion defined by

$$G^{-1}(\omega, \vec{p}) := \begin{pmatrix} \omega - \frac{p^2}{2m} + \mu - M & \Delta_s^* + \vec{\sigma} \cdot \vec{\Delta}_v^* \\ \Delta_s + \vec{\sigma} \cdot \vec{\Delta}_v & \omega - \lambda \end{pmatrix}, \quad (2.12)$$

$$\det G^{-1}(\omega, \vec{p}) \equiv \prod_{i=1}^4 [\omega - \omega_i(\vec{p})]. \quad (2.13)$$

In this paper, we set Λ to be unity. The first, second, and third terms in the right-hand side of eq. (2.11) are potential, vacuum, and thermal contributions to Ω , respectively.

2.2 Energy-momentum dispersion

Solving $\det G^{-1}(\omega_i, \vec{p}) = 0$, we obtain the energy-momentum dispersion

$$\omega_{i=1,\dots,4} = \mathcal{E}_\pm \pm \sqrt{\mathcal{E}_\pm^2 + |\Delta_s|^2 + |\vec{\Delta}_v|^2 \pm \sqrt{(|\Delta_s|^2 + |\vec{\Delta}_v|^2)^2 - |\Delta_s^2 - \vec{\Delta}_v \cdot \vec{\Delta}_v|^2}}, \quad (2.14)$$

where

$$\mathcal{E}_\pm := \frac{1}{2} \left[\left(\frac{p^2}{2m} - \mu + M \right) \pm \lambda \right]. \quad (2.15)$$

Since ω_i is invariant under rotation and depends on the phases of the condensations only through their difference, we set an ansatz

$$\Delta_s = |\Delta_s|, \quad \vec{\Delta}_v = |\Delta_v| e^{i\theta} \hat{n}, \quad (2.16)$$

where θ is the phase difference between the Kondo condensations and \hat{n} is a unit vector. Then, we obtain

$$\omega_{i=1,\dots,4} = \mathcal{E}_\pm \pm \sqrt{\mathcal{E}_\pm^2 + |\Delta_s|^2 + |\Delta_v|^2 \pm 2|\Delta_s||\Delta_v| \cos \theta}. \quad (2.17)$$

M effectively decreases μ , ω_i is invariant under $|\Delta_s| \leftrightarrow |\Delta_v|$, $|\Delta_{s,v}|$ open the hybridization gap, and the spin degeneracy is broken when $\theta \neq \pm\pi/2$ and $|\Delta_{s,v}| \neq 0$ (see eqs. (2.15) and (2.17)). Figure 1 shows the energy-momentum dispersion and the hybridization gap.

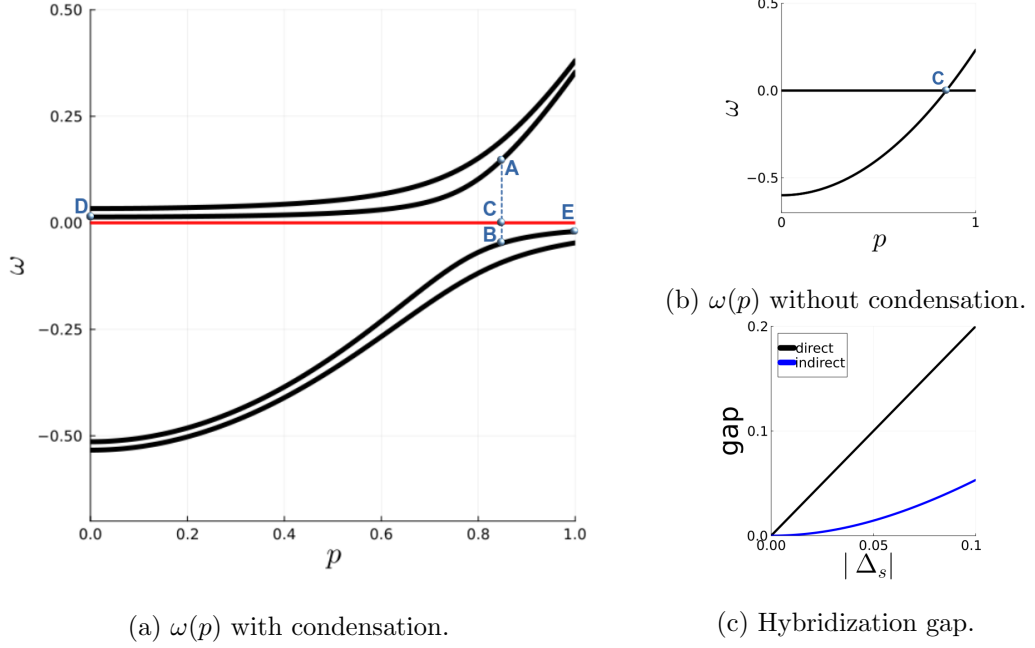


Figure 1: Energy-momentum dispersion and the hybridization gap. $m = \mu = 0.6$, $\lambda = 10^{-8}$. (a,b) Black lines represent ω_i and red lines represent the Fermi level. We used $M = 0.1$, $|\Delta_s| = 0.1$, $|\Delta_v| = 0.05$, $\theta = 1$ for (a), while $M = 0$, $|\Delta_s| = 0$, $|\Delta_v| = 0$, $\theta = 0$ for (b). Point C is the band crossing point before the gap opening. Point A (B) is the intersection of the vertical line extending from C and the upper (lower) band. The gap between A and B is called the direct gap. Point D (E) is at the bottom (top) of the upper (lower) band. The gap between D and E is called the indirect gap. (c) $M = 0$, $|\Delta_v| = 0$. Black and blue lines show the direct and indirect gaps, respectively. The direct gap is approximately linear in $|\Delta_s|$, while the indirect gap is quadratic.

2.3 Formation of the Kondo condensation

Given fixed parameters $\pi := (m, \mu, \lambda, g_l, g_s, g_v, \beta)$, the thermodynamic potential Ω is a function of four real variables M , $|\Delta_s|$, $|\Delta_v|$, and θ :

$$\Omega \equiv \Omega_{\pi}(M, |\Delta_s|, |\Delta_v|, \theta). \quad (2.18)$$

Minimizing the function Ω_{π} , we can obtain $(M, |\Delta_s|, |\Delta_v|, \theta)$ at thermal equilibrium for given parameters π :

$$\min \Omega_{\pi} \equiv \Omega_{\pi}(M_{\text{eq}}(\pi), |\Delta_s|_{\text{eq}}(\pi), |\Delta_v|_{\text{eq}}(\pi), \theta_{\text{eq}}(\pi)). \quad (2.19)$$

To check the stability of our mean field model, consider Ω with large condensation Δ :

$$\begin{aligned} \Omega_{\text{large } \Delta} = & \underbrace{\left(\frac{M^2}{2g_l} + \frac{|\Delta_s|^2}{g'_s} + \frac{|\Delta_v|^2}{g'_v} \right)}_{O(\Delta^2)} + \underbrace{\frac{1}{V} \sum_{|\vec{p}| < \Lambda} \sum_{i=1}^4 \left(-\frac{1}{2} |\omega_i(\vec{p})| \right)}_{O(\Delta^1)} \\ & + \underbrace{\frac{1}{V} \sum_{|\vec{p}| < \Lambda} \sum_{i=1}^4 \left\{ -\frac{1}{\beta} \ln \left[1 + e^{-\beta |\omega_i(\vec{p})|} \right] \right\}}_{O(\Delta^0)}. \end{aligned} \quad (2.20)$$

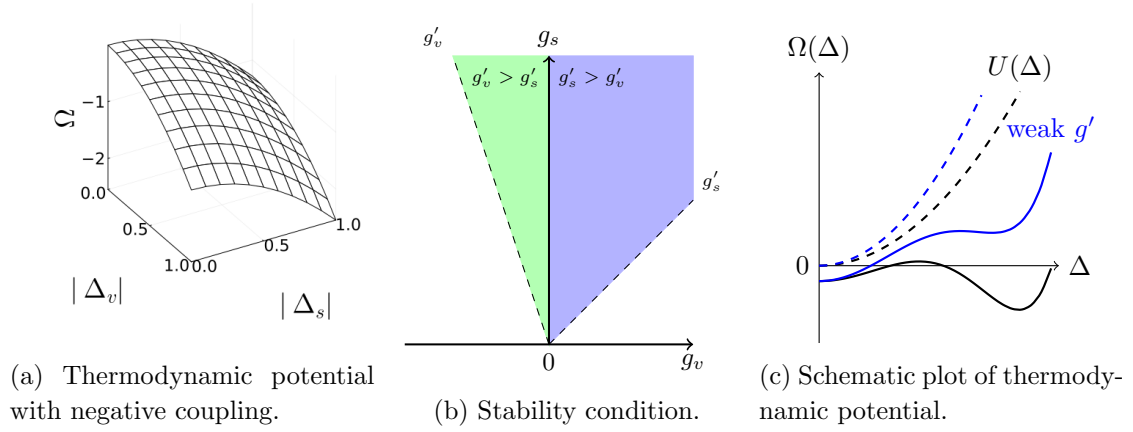


Figure 2: (a) $m = \mu = 0.6$, $\lambda = 10^{-8}$, $g_l = 0.01$, $g'_s = g'_v = -0.8$, $T = 0$, $M = 0$, $\theta = \pi/2$. (b) On green (blue) region, $g'_v > g'_s > 0$ ($g'_s > g'_v > 0$). At the boundary between the green and blue regions, $g'_s = g'_v$, or equivalently, $g_v = 0$. On the green and blue regions, the stability condition $g'_s, g'_v > 0$ holds. (c) Dashed lines are for $U(\Delta) \sim \Delta^2/g'$, solid lines are for $\Omega(\Delta) \sim \Delta^2/g' - \frac{1}{2} \int |\omega_\Delta|$, and blue lines are for weak g' .

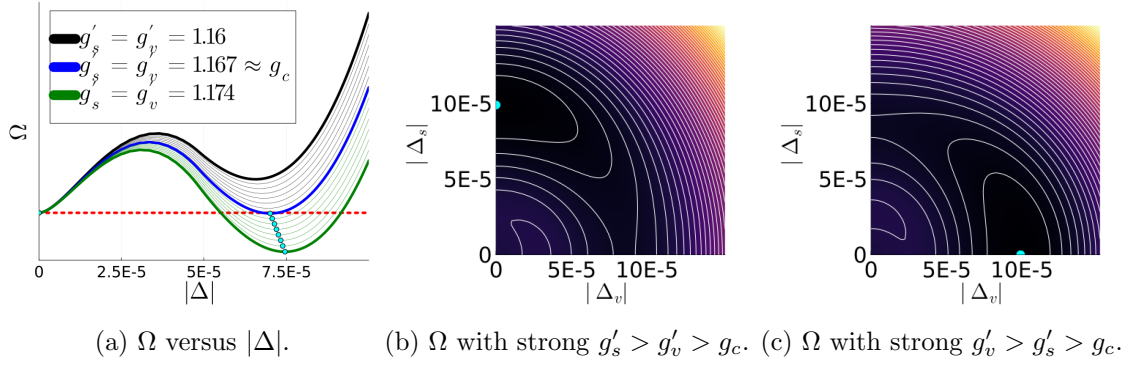


Figure 3: Thermodynamic potential at zero temperature. $m = \mu = 0.6$, $\lambda = 10^{-8}$, $g_l = 0.01$, $T = 0$, $M = 0 \approx M_{\text{eq}}$, $\theta = \pi/2 \approx \theta_{\text{eq}}$. Cyan points and line represent the minima of Ω . (a) shows Ω versus $|\Delta| := \sqrt{|\Delta_s|^2 + |\Delta_v|^2}$ for various $g'_s = g'_v$. (b,c) The brighter it is, the higher the value of Ω . (b) $g'_s = 1.21$, $g'_v = 1.19$. (c) $g'_s = 1.19$, $g'_v = 1.21$.

For large Δ , the potential contribution to Ω , the first term in the right-hand side of eq. (2.20), is dominant relative to other contributions. Apart from that, for Ω to have a minimum with finite Δ , Ω must not go to negative infinity as Δ goes to infinity. Therefore, g_l , g'_s , and g'_v should be positive so that the potential contribution does not go to negative infinity (see eq. (2.10)). Figure 2a shows the thermodynamic potential in the case of $g'_{s,v} < 0$. We can rewrite the stability condition $g'_{s,v} > 0$ in terms of $g_{s,v}$ in eq. (2.1) as $g_s > -3g_v$, $g_s > g_v$ (see figure 2b). For the above stability condition to hold, we need nonzero positive g_s .

To analyze the effects of the contributions to Ω and the heavy-light coupling g' at zero

temperature qualitatively, consider

$$\Omega_{T=0} = \underbrace{\frac{M^2}{2g_l} + \frac{|\Delta_s|^2}{g'_s} + \frac{|\Delta_v|^2}{g'_v}}_{\Delta^2/g'} + \underbrace{\frac{1}{V} \sum_{|\vec{p}| < \Lambda} \sum_{i=1}^4 \left(-\frac{1}{2} |\omega_i(\vec{p})| \right)}_{-\frac{1}{2} \int |\omega_\Delta|}. \quad (2.21)$$

Without the vacuum contribution $-\frac{1}{2} \int |\omega_\Delta|$, minimization of the potential contribution Δ^2/g' gives $\Delta = 0$ (see the dashed lines in figure 2c). Therefore, $-\frac{1}{2} \int |\omega_\Delta|$ is important to make a new vacuum with nonzero Kondo condensation Δ . If g' is weak, Δ^2/g' is dominant so that there is no way to make a new vacuum (see the solid blue line in figure 2c).

Figure 3 shows Ω at $T = 0$ with fixed $M = M_{\text{eq}} = 0$, $\theta = \theta_{\text{eq}} = \pi/2$. When $g'_{s,v}$ are weak, the Kondo condensations do not arise (see the black line in figure 3a). However, as we increase $g'_{s,v}$, there is a new vacuum, where the Kondo condensation is nonzero (see the blue line in figure 3a). Since the thermodynamic potential is invariant under rotation on the $|\Delta_s|$ - $|\Delta_v|$ plane if $g'_s = g'_v$ and $\theta = \pi/2$ (see eqs. (2.10), (2.11), and (2.17)), there are infinitely many degenerate minima. The critical coupling constant is $g_c \approx 1.167$, and the formation of the Kondo condensation is a first-order quantum phase transition (see figure 3a). If we change $g'_{s,v}$ so that $g'_s > g'_v$, then there is a unique minimum with $|\Delta_s| \neq 0$ but $|\Delta_v| = 0$ (see figure 3b). In the opposite case $g'_s < g'_v$, only $|\Delta_v|$ forms (see figure 3c). We also perform the finite-temperature calculation in the case of $g'_s > g'_v$ (see the blue region in figure 2b); and show that, if the temperature is low and the heavy-light coupling is strong, only the scalar-type Kondo condensation forms so that our model is reduced to a Anderson-like model with lattice (see appendix B).

3 Holographic Kondo lattice model

3.1 Setup

Consider a metric field g , a $U(1)$ gauge field A , two neutral real scalar fields $\Phi_{s,\text{ps}}$, and two probe spinor fields $\psi^{(1,2)}$ in AdS_4 :

$$S_{\text{tot}} = S_{\text{bg}} + S_{\text{spin}}, \quad (3.1)$$

$$S_{\text{bg}} = S_{\text{bg,bdy}} + \int d^4x \sqrt{-g} \left(R + \frac{6}{L^2} - \frac{1}{4} F_{\mu\nu} F^{\mu\nu} \right) + \int d^4x \sqrt{-g} [-(\partial_\mu \Phi_s)(\partial^\mu \Phi_s) - m_s^2 \Phi_s^2 - (\partial_\mu \Phi_{\text{ps}})(\partial^\mu \Phi_{\text{ps}}) - m_{\text{ps}}^2 \Phi_{\text{ps}}^2], \quad (3.2)$$

$$S_{\text{spin}} = S_{\text{spin,bdy}} + \sum_{j=1}^2 \int d^4x \sqrt{-g} i \bar{\psi}^{(j)} \left[\frac{1}{2} \left(\overrightarrow{\not{D}}^{(j)} - \overleftarrow{\not{D}}^{(j)} \right) - m_j \right] \psi^{(j)} + \int d^4x \sqrt{-g} \begin{pmatrix} \bar{\psi}^{(1)} \\ \bar{\psi}^{(2)} \end{pmatrix}^T \begin{pmatrix} g_1 \Phi_{\text{ps}} \cdot \Gamma^5 & V \Phi_s \cdot i \mathbb{I}_4 \\ V \Phi_s \cdot i \mathbb{I}_4 & g_2 \Phi_s \cdot i \mathbb{I}_4 \end{pmatrix} \begin{pmatrix} \psi^{(1)} \\ \psi^{(2)} \end{pmatrix}, \quad (3.3)$$

$$S_{\text{spin,bdy}} = \frac{1}{2} \int d^3x \sqrt{-h} [\bar{\psi}^{(1)} (i \mathbb{I}_4) \psi^{(1)} + \bar{\psi}^{(2)} \Gamma^{\underline{xy}} \psi^{(2)}], \quad (3.4)$$

where

$$\mathcal{D}^{(j)} = \Gamma^a e_a{}^B \left(\partial_B + \frac{1}{4} \omega_{Bcd} \Gamma^{cd} - i q_j A_B \right), \quad h = g g^{uu}, \quad (3.5)$$

$$L = 1, \quad \bar{\psi}^{(j)} = \psi^{(j)\dagger} \Gamma^{\mathbf{t}}, \quad (3.6)$$

$$\Gamma^{\mathbf{t}} = \sigma_1 \otimes i\sigma_2 = \begin{pmatrix} 0 & i\sigma_2 \\ i\sigma_2 & 0 \end{pmatrix}, \quad \Gamma^{\mathbf{x}} = \sigma_1 \otimes \sigma_1 = \begin{pmatrix} 0 & \sigma_1 \\ \sigma_1 & 0 \end{pmatrix}, \quad (3.7)$$

$$\Gamma^{\mathbf{y}} = \sigma_1 \otimes \sigma_3 = \begin{pmatrix} 0 & \sigma_3 \\ \sigma_3 & 0 \end{pmatrix}, \quad \Gamma^{\mathbf{u}} = \sigma_3 \otimes \sigma_0 = \begin{pmatrix} \sigma_0 & 0 \\ 0 & -\sigma_0 \end{pmatrix}, \quad (3.8)$$

$$\Gamma^5 = i\Gamma^{\mathbf{t}}\Gamma^{\mathbf{x}}\Gamma^{\mathbf{y}}\Gamma^{\mathbf{u}}, \quad \Gamma^{ab} = \frac{1}{2}[\Gamma^a, \Gamma^b]. \quad (3.9)$$

$m_{\text{s,ps}}$ and $m_{1,2}$ are the bulk masses of $\Phi_{\text{s,ps}}$ and $\psi^{(1,2)}$, respectively. We list the motivation for the above action in the following:

- $g_1 \bar{\psi}^{(1)}(\Phi_{\text{ps}} \cdot \Gamma^5) \psi^{(1)}$ makes a hyperbolic spectrum of the light fermion (to see why we have not chosen the scalar-type interaction, see appendix D).
- We consider the standard-mixed quantization to flatten the spectrum of the heavy fermion dual to $\psi^{(2)}$ (see eq. (3.4) and refs. [70, 71, 83]). The flat spectrum comes from the cancellation of the spinor components making the compact localized states (CLS) [71, 84].
- $g_2 \bar{\psi}^{(2)}(\Phi_{\text{s}} \cdot i\mathbb{I}_4) \psi^{(2)}$ isolates the flat band from others (see appendix D and ref. [71]).
- $V \bar{\psi}^{(1)}(\Phi_{\text{s}} \cdot i\mathbb{I}_4) \psi^{(2)}$ hybridizes the light and heavy fermions.

It turns out that the fermion spectral function depends on the mass of Φ_{ps} very sensitively. Let $\Phi_{\text{ps}} \sim u^\alpha + \dots$ near the boundary. If $\alpha > 1$ (equivalently if $m_{\text{ps}}^2 < -2$), then the fermion spectral function has sharp towers of hyperbolic bands, while for $\alpha \leq 1$ (equivalently if $m_{\text{ps}}^2 \geq -2$), then the fermion spectral function has fuzzy filled bands with hyperbolic envelope. Since we want to imitate the dispersive band like weakly interacting case, we couple the dispersive fermion to the pseudo-scalar with $m_{\text{ps}}^2 = -9/4$. The specific value $-9/4$ is just to make the power as a simplest possible under the constraint.

3.2 Background fields

We first consider the background fields only by neglecting the probe spinor fields:

$$\begin{aligned} S_{\text{bg}} = S_{\text{bg, bdy}} + \int d^4x \sqrt{-g} \left(R + \frac{6}{L^2} - \frac{1}{4} F_{\mu\nu} F^{\mu\nu} \right) \\ + \int d^4x \sqrt{-g} [-(\partial_\mu \Phi_{\text{s}})(\partial^\mu \Phi_{\text{s}}) - m_{\text{s}}^2 \Phi_{\text{s}}^2 - (\partial_\mu \Phi_{\text{ps}})(\partial^\mu \Phi_{\text{ps}}) - m_{\text{ps}}^2 \Phi_{\text{ps}}^2]. \end{aligned} \quad (3.10)$$

When we choose $m_{\text{s}}^2 = -2$, $m_{\text{ps}}^2 = -9/4$ and take ansatz

$$ds^2 = \frac{1}{u^2} [-f(u) \chi(u) dt^2 + dx^2 + dy^2] + \frac{du^2}{f(u)u^2}, \quad (3.11)$$

$$A = A_t(u) dt, \quad \Phi_{\text{s}} = \Phi_{\text{s}}(u), \quad \Phi_{\text{ps}} = \Phi_{\text{ps}}(u), \quad (3.12)$$

the equations of motion of the background fields $\delta S_{\text{bg}} = 0$ read

$$f' - \left(\frac{3}{u} + \frac{u\Phi_s'^2}{2} + \frac{u\Phi_{\text{ps}}'^2}{2} \right) f + \frac{3}{u} + \frac{\Phi_s^2}{u} + \frac{9\Phi_{\text{ps}}^2}{8u} - \frac{u^3 A_t'^2}{4\chi} = 0, \quad (3.13)$$

$$\chi' + (u\Phi_s'^2 + u\Phi_{\text{ps}}'^2)\chi = 0, \quad (3.14)$$

$$A_t'' - \frac{\chi'}{2\chi} A_t' = 0, \quad (3.15)$$

$$\Phi_s'' + \left(\frac{f'}{f} + \frac{\chi'}{2\chi} - \frac{2}{u} \right) \Phi_s' + \frac{2}{u^2 f} \Phi_s = 0, \quad (3.16)$$

$$\Phi_{\text{ps}}'' + \left(\frac{f'}{f} + \frac{\chi'}{2\chi} - \frac{2}{u} \right) \Phi_{\text{ps}}' + \frac{9}{4u^2 f} \Phi_{\text{ps}} = 0, \quad (3.17)$$

and the Hawking temperature is given by

$$T := \frac{\sqrt{\chi(u_h)} |f'(u_h)|}{4\pi}. \quad (3.18)$$

The asymptotic behavior near the boundary is as follows:

$$A_t \approx \mu - \rho u, \quad (3.19)$$

$$\Phi_s \approx \Phi_{s,-} u + \Phi_{s,+} u^2, \quad (3.20)$$

$$\Phi_{\text{ps}} \approx \Phi_{\text{ps},-} u^{3/2} \ln u + \Phi_{\text{ps},+} u^{3/2}, \quad (3.21)$$

where μ is the chemical potential, $\Phi_{s/\text{ps},-}$ are the sources of $\Phi_{s/\text{ps}}$. We impose the following boundary condition

$$f(u_h) = 0, \quad \chi(0) = 1, \quad (3.22)$$

$$\mu = 0.1, \quad A(u_h) = 0, \quad (3.23)$$

$$\Phi_{s,-} = 0.1, \quad \Phi_s(u_h) = \text{finite}, \quad (3.24)$$

$$\Phi_{\text{ps},-} = 0.1, \quad \Phi_{\text{ps}}(u_h) = \text{finite}, \quad (3.25)$$

where we have set all control parameters μ , $\Phi_{s,-}$, and $\Phi_{\text{ps},-}$ as 0.1. In numerical calculation, we cut the domain to be $u \in [\epsilon, u_h - \epsilon]$ with some small value ϵ , and then set boundary condition as follows:

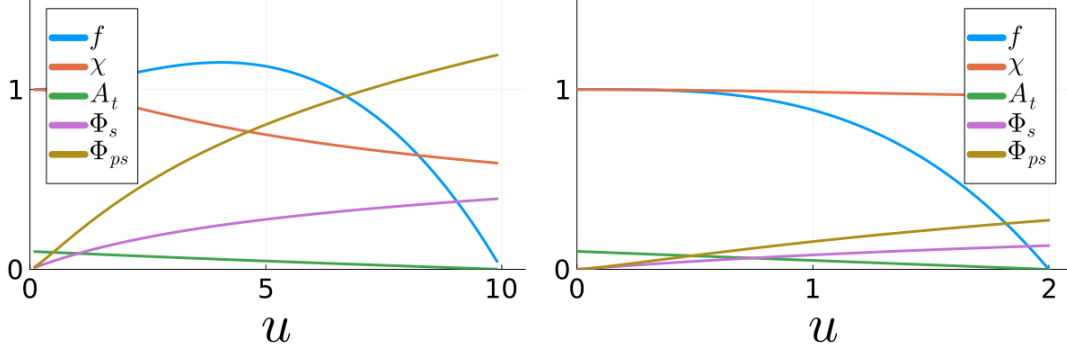
$$f(u_h - \epsilon) + \epsilon f'(u_h - \epsilon) = 0, \quad \chi(\epsilon) - \epsilon \chi'(\epsilon) - 1 = 0, \quad (3.26)$$

$$A_t(\epsilon) - \epsilon A_t'(\epsilon) - \mu = 0, \quad A_t(u_h - \epsilon) + \epsilon A_t'(u_h - \epsilon) = 0, \quad (3.27)$$

$$\Phi_s(\epsilon) - \frac{1}{2} \epsilon \Phi_s'(\epsilon) - \frac{1}{2} \Phi_{s,-} \epsilon = 0, \quad \epsilon^2 \Phi_s''(u_h - \epsilon) = 0, \quad (3.28)$$

$$\Phi_{\text{ps}}(\epsilon) - \frac{2}{3} \epsilon \Phi_{\text{ps}}'(\epsilon) - \frac{2}{3} \Phi_{\text{ps},-} \epsilon^{3/2} = 0, \quad \epsilon^2 \Phi_{\text{ps}}''(u_h - \epsilon) = 0. \quad (3.29)$$

Figure 4 shows the result of the numerical calculation for the background fields.



(a) At low temperature ($u_h = 10, T \approx 0.026$). (b) At high temperature ($u_h = 2, T \approx 0.121$).

Figure 4: Background fields.

3.3 Probe spinor fields

3.3.1 Equations of motion of the probe spinor fields

After solving the background fields, we consider the probe spinors:

$$S_{\text{spin}} = S_{\text{spin, bdy}} + \sum_{j=1}^2 \int d^4x \sqrt{-g} i \bar{\psi}^{(j)} \left[\frac{1}{2} \left(\vec{D}^{(j)} - \overleftarrow{D}^{(j)} \right) - m_j \right] \psi^{(j)} + \int d^4x \sqrt{-g} \begin{pmatrix} \bar{\psi}^{(1)} \\ \bar{\psi}^{(2)} \end{pmatrix}^T \begin{pmatrix} g_1 \Phi_{ps} \cdot \Gamma^5 & V \Phi_s \cdot i \mathbb{I}_4 \\ V \Phi_s \cdot i \mathbb{I}_4 & g_2 \Phi_s \cdot i \mathbb{I}_4 \end{pmatrix} \begin{pmatrix} \psi^{(1)} \\ \psi^{(2)} \end{pmatrix}, \quad (3.30)$$

with boundary action

$$S_{\text{spin, bdy}} = \frac{1}{2} \int d^3x \sqrt{-h} [\bar{\psi}^{(1)} \Gamma^{(1)} \psi^{(1)} + \bar{\psi}^{(2)} \Gamma^{(2)} \psi^{(2)}], \quad (3.31)$$

where $\Gamma^{(j)}$ are some complex 4×4 matrices that can be written in the block-diagonal form:

$$\Gamma^{(j)} \equiv \begin{pmatrix} \gamma_{11}^{(j)} & 0 \\ 0 & \gamma_{22}^{(j)} \end{pmatrix}. \quad (3.32)$$

Assuming that the background fields are not affected by the probe spinor fields, we have

$$\delta S_{\text{spin}} = (\text{equations of motion term}) + \sum_{j=1}^2 \frac{1}{2} \int d^3x \sqrt{-h} [\bar{\psi}^{(j)} (\Gamma^{(j)} + i \Gamma^{\underline{u}}) (\delta \psi^{(j)}) + (\delta \bar{\psi}^{(j)}) (\Gamma^{(j)} - i \Gamma^{\underline{u}}) \psi^{(j)}], \quad (3.33)$$

where the equations of motion of the probe spinors are given by

$$\left[\begin{pmatrix} \vec{D} - m_1 & 0 \\ 0 & \vec{D} - m_2 \end{pmatrix} - i \begin{pmatrix} g_1 \Phi_{ps} \cdot \Gamma^5 & V \Phi_s \cdot i \mathbb{I}_4 \\ V \Phi_s \cdot i \mathbb{I}_4 & g_2 \Phi_s \cdot i \mathbb{I}_4 \end{pmatrix} \right] \begin{pmatrix} \psi^{(1)} \\ \psi^{(2)} \end{pmatrix} = 0. \quad (3.34)$$

Substituting $\psi^{(j)} = (-h)^{-1/4} \phi^{(j)}$ to the equations of motion, we get

$$[\Gamma^a e_a^B (\partial_B - iq_1 A_B) - m_1 - ig_1 \Phi_{\text{ps}} \Gamma^5] \phi^{(1)} + V \Phi_s \phi^{(2)} = 0, \quad (3.35)$$

$$V \Phi_s \phi^{(1)} + [\Gamma^a e_a^B (\partial_B - iq_2 A_B) - m_2 + g_2 \Phi_s] \phi^{(2)} = 0. \quad (3.36)$$

Then, taking

$$\phi^{(j)}(t, x, y, u) = \int \frac{d^3 k}{(2\pi)^3} e^{-i\omega t + i\vec{k} \cdot \vec{x}} \phi_k^{(j)}(u) \quad [k \equiv (\omega, \vec{k}) \equiv (\omega, k_x, k_y)], \quad (3.37)$$

we obtain

$$\partial_u \phi_k^{(1)} + \Gamma^{\mathbb{U}} \left[\frac{-i(\omega + q_1 A_t) \Gamma^{\mathbb{T}}}{f\sqrt{\chi}} + \frac{ik_x \Gamma^{\mathbb{X}} + ik_y \Gamma^{\mathbb{Y}}}{\sqrt{f}} + \frac{-m_1 - ig_1 \Phi_{\text{ps}} \Gamma^5}{u\sqrt{f}} \right] \phi_k^{(1)} + \frac{V \Phi_s \Gamma^{\mathbb{U}}}{u\sqrt{f}} \phi_k^{(2)} = 0, \quad (3.38)$$

$$\partial_u \phi_k^{(2)} + \frac{V \Phi_s \Gamma^{\mathbb{U}}}{u\sqrt{f}} \phi_k^{(1)} + \Gamma^{\mathbb{U}} \left[\frac{-i(\omega + q_2 A_t) \Gamma^{\mathbb{T}}}{f\sqrt{\chi}} + \frac{ik_x \Gamma^{\mathbb{X}} + ik_y \Gamma^{\mathbb{Y}}}{\sqrt{f}} + \frac{-m_2 + g_2 \Phi_s}{u\sqrt{f}} \right] \phi_k^{(2)} = 0. \quad (3.39)$$

3.3.2 Probe spinor fields near the boundary

The asymptotic behavior of the probe spinor fields near the boundary is as follows:

$$\phi_k^{(j)} \approx \begin{pmatrix} A_k^{(j)} u^{m_j} + B_k^{(j)} u^{1-m_j} \\ C_k^{(j)} u^{1+m_j} + D_k^{(j)} u^{-m_j} \end{pmatrix}. \quad (3.40)$$

We assume $0 < |m_j| < 1/2$ so that the leading asymptotic behavior is

$$\phi_k^{(j)} \approx \begin{pmatrix} A_k^{(j)} u^{m_j} \\ D_k^{(j)} u^{-m_j} \end{pmatrix}. \quad (3.41)$$

Define

$$\Gamma_{\pm}^{(j)} := \frac{1}{2} (\Gamma^{(j)} \pm i \Gamma^{\mathbb{U}}), \quad \Gamma^{\mathbb{T}} \Gamma_+ \equiv Q^{(j)\dagger} P^{(j)}, \quad (3.42)$$

$$\varphi_k^{(j)} := \begin{pmatrix} A_k^{(j)} \\ D_k^{(j)} \end{pmatrix}, \quad \bar{\varphi}_k^{(j)} := \varphi_k^{(j)} \Gamma^{\mathbb{T}}, \quad (3.43)$$

$$\bar{A}_k^{(j)} := A_k^{(j)\dagger} i\sigma_2, \quad \bar{D}_k^{(j)} := D_k^{(j)\dagger} i\sigma_2, \quad (3.44)$$

$$C_k := \begin{pmatrix} C_k^{(1)} \\ C_k^{(2)} \end{pmatrix} := \begin{pmatrix} Q^{(1)} \varphi_k^{(1)} \\ Q^{(2)} \varphi_k^{(2)} \end{pmatrix}, \quad J_k := \begin{pmatrix} J_k^{(1)} \\ J_k^{(2)} \end{pmatrix} := \begin{pmatrix} P^{(1)} \varphi_k^{(1)} \\ P^{(2)} \varphi_k^{(2)} \end{pmatrix}, \quad (3.45)$$

$$C_k \equiv G_k J_k \quad (\forall J_k), \quad (3.46)$$

where G_k can be determined by introducing the infalling boundary condition and solving the equations of motion (see appendix C). Assuming

$$\text{rank } \Gamma_{\pm}^{(j)} = 2, \quad \Gamma_-^{(j)} = \Gamma^{\mathbb{T}} \Gamma_+^{(j)\dagger} \Gamma^{\mathbb{T}}, \quad (3.47)$$

and substituting the solution to S_{spin} , we have

$$\begin{aligned}
\underline{S}_{\text{spin}} &:= S_{\text{spin}} \Big|_{\psi=\psi_{\text{sol}}, u \rightarrow 0} \\
&= \sum_{j=1}^2 \frac{1}{2} \int d^3x \frac{d^3k}{(2\pi)^3} \frac{d^3k'}{(2\pi)^3} e^{-i(\omega-\omega')t + i(\vec{k}-\vec{k}') \cdot \vec{x}} \phi_k^{(j)\dagger} \Gamma^{\text{t}} \Gamma^{(j)} \phi_{k'}^{(j)} \Big|_{\phi=\phi_{\text{sol}}, u \rightarrow 0} \\
&= \sum_{j=1}^2 \frac{1}{2} \int \frac{d^3k}{(2\pi)^3} \begin{pmatrix} A_k^{(j)} u^{m_j} \\ D_k^{(j)} u^{-m_j} \end{pmatrix}^{\dagger} \Gamma^{\text{t}} \begin{pmatrix} \gamma_{11}^{(j)} & 0 \\ 0 & \gamma_{22}^{(j)} \end{pmatrix} \begin{pmatrix} A_k^{(j)} u^{m_j} \\ D_k^{(j)} u^{-m_j} \end{pmatrix} \Big|_{u \rightarrow 0} \\
&= \sum_{j=1}^2 \frac{1}{2} \int \frac{d^3k}{(2\pi)^3} (\bar{A}_k^{(j)} \gamma_{22}^{(j)} D_k^{(j)} + \bar{D}_k^{(j)} \gamma_{11}^{(j)} A_k^{(j)}) \tag{3.48} \\
&= \sum_{j=1}^2 \frac{1}{2} \int \frac{d^3k}{(2\pi)^3} (\bar{\varphi}_k^{(j)} \Gamma_+^{(j)} \varphi_k^{(j)} + \bar{\varphi}_k^{(j)} \Gamma^{\text{t}} \Gamma_+^{(j)\dagger} \Gamma^{\text{t}} \varphi_k^{(j)}) \\
&= \frac{1}{2} \int \frac{d^3k}{(2\pi)^3} (C_k^{\dagger} J_k + J_k^{\dagger} C_k) \\
&= \frac{1}{2} \int \frac{d^3k}{(2\pi)^3} (J_k^{\dagger} G_k^{\dagger} J_k + J_k^{\dagger} G_k J_k).
\end{aligned}$$

Then, using the Gubser-Klebanov-Polyakov-Witten relation [39, 40], we can show that G_k is the Green's function of the boundary operator dual to the probe spinor fields [74].

3.4 Spectral function and density of states

After calculating the Green's function G_k^{SM} in the standard-mixed quantization, we consider the spectral function $A(\omega, \vec{k})$ and the density of states $g(\omega)$ that are defined by

$$A(\omega, \vec{k}) := \lim_{\delta \rightarrow 0^+} 2 \text{Im tr } G_{(\omega+i\delta, \vec{k})}^{\text{SM}}, \tag{3.49}$$

$$g(\omega) := \int_{|\vec{k}| < 1} \frac{dk_x dk_y}{(2\pi)^2} A(\omega, \vec{k}) = \frac{1}{2\pi} \int_0^1 dk k A(\omega, k), \tag{3.50}$$

where we have introduced momentum cutoff $|\vec{k}| < \Lambda = 1$ and used the rotational symmetry of the system.

Figure 5 shows the result of numerical calculation with $q_1 = 23.5$, $q_2 = 0$, $g_1 = 10$, $g_2 = 15$, and $m_1 = m_2 = 0^+$. δ must be 0^+ in principle, but we set $\delta = 10^{-3}$ in the numerical calculation. Without V , there exist hyperbolic and flat spectra independently (see figures 5a and 5c). As we turn on V , the hybridization gap opens (see figures 5b and 5d). At high temperatures, the spectra spread wide and the hybridization gap becomes a pseudogap, an incomplete gap where the density of states does not touch zero (see figures 5g and 5h). The spectra and density of states are asymmetric under $\omega \rightarrow -\omega$ unlike the holographic Kondo model for random impurities [27].

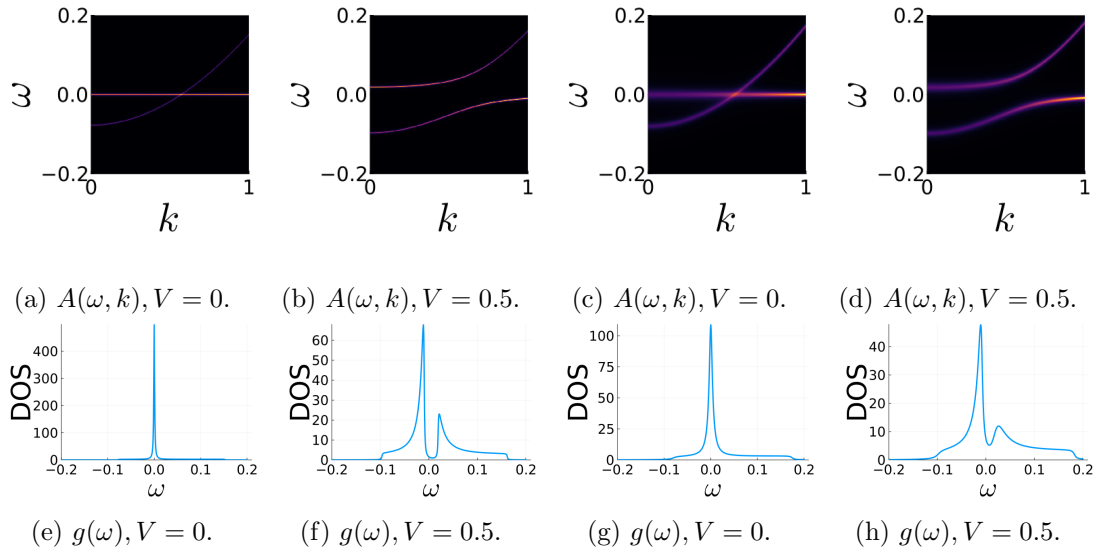


Figure 5: Holographic Kondo lattice model. The upper four figures (a,b,c,d) shows the spectral function $A(\omega, k)$ corresponding to the lower four figures (e,f,g,h) of the density of states $g(\omega)$, respectively. We used $u_h = 10, T \approx 0.026$ for the left four figures (a,b,e,f), while $u_h = 2, T \approx 0.121$ for the right four figures (c,d,g,h). The brighter points in (a,b,c,d) represent higher values of $A(\omega, k)$.

4 Conclusion

We start from a non-relativistic field theory model with s - d interaction based on the Kondo model. Our model can be transformed into an Anderson-like model using the Fierz identity and the mean field approximation, which is more straightforward than the Schrieffer-Wolff transformation. We note that we must consider the instability and add a scalar-type s - d interaction term to stabilize the mean field calculation. M shifts the dispersion of the light fermion, while the Kondo condensation hybridizes the light and heavy fermions. The spin degeneracy is broken when there are two types of Kondo condensation. Our numerical calculation of the mean field model shows that the Kondo condensation forms at low temperatures if the s - d mixing is strong. The type of the Kondo condensation is determined by the inequality of vector- and scalar-type coupling constants. If the vector-type Kondo condensation does not arise, our mean field model is reduced to a lattice version of the Anderson model. The formation of the Kondo condensation at zero temperature with varying s - d mixing exemplifies the first-order quantum phase transition.

Then, based on the result of the non-relativistic mean field model, we propose an explicitly-symmetry-broken holographic Kondo lattice model using two-flavor spinors in the standard-mixed quantization. The spinors in the standard and mixed quantizations give conduction and flat spectra, respectively. We calculate the fermionic spectral function and density of states and show that the inter-flavor coupling hybridizes the conduction and flat spectra like the Kondo condensation.

There are some of the things we have left out. We have yet to consider the effect of an external magnetic field, which is crucial to comparing the theoretical result with the

experiment in ref. [27]. On the other hand, the explicitly-symmetry-broken holographic model in this paper cannot explain the formation of the Kondo condensation. Hence, it would be interesting to study the Kondo lattice model with external fields in strong coupling regions or to construct spontaneous-symmetry-broken holographic Kondo lattice models by including non-linear self-coupling of scalar field or coupling between scalar field with another. We will consider these issues in future works.

Acknowledgments

This work is supported by Mid-career Researcher Program through the National Research Foundation of Korea grant No. NRF-2021R1A2B5B02002603, RS-2023-00218998 and NRF-2022H1D3A3A01077468. We thank the APCTP for the hospitality during the focus program, where part of this work was discussed.

A Thermodynamic potential of the non-relativistic mean field model

The partition function is given by

$$\mathcal{Z} = \int \mathcal{D}\Psi^\dagger \mathcal{D}\Psi \exp \left[- \int_0^\beta d\tau \int d^3x (-\Psi^\dagger D_E \Psi + U) \right], \quad (\text{A.1})$$

where

$$D_E := \begin{pmatrix} -\frac{\partial}{\partial \tau} + \frac{\nabla^2}{2m} + \mu - M & \Delta_s^* + \vec{\sigma} \cdot \vec{\Delta}_v^* \\ \Delta_s + \vec{\sigma} \cdot \vec{\Delta}_v & -\frac{\partial}{\partial \tau} - \lambda \end{pmatrix}. \quad (\text{A.2})$$

Since U is independent of \vec{x} , τ , Ψ , and Ψ^\dagger ,

$$\ln \mathcal{Z} = -\beta V U + \ln \left[\int \mathcal{D}\Psi^\dagger \mathcal{D}\Psi \exp \left(\int_0^\beta d\tau \int d^3x \Psi^\dagger D_E \Psi \right) \right]. \quad (\text{A.3})$$

Performing the Fourier transform,

$$\Psi(\tau, \vec{x}) = \sum_{n=-\infty}^{\infty} \sum_{|\vec{p}| < \Lambda} e^{i(\nu_n \tau + \vec{p} \cdot \vec{x})} \Psi_n(\vec{p}), \quad (\text{A.4})$$

$$\Psi^\dagger(\tau, \vec{x}) = \sum_{n=-\infty}^{\infty} \sum_{|\vec{p}| < \Lambda} e^{-i(\nu_n \tau + \vec{p} \cdot \vec{x})} \Psi_n^\dagger(\vec{p}), \quad (\text{A.5})$$

where $\nu_n := (2n + 1)\pi/\beta$ is the Matsubara frequency, we obtain

$$\begin{aligned}
\ln \mathcal{Z} &= -\beta VU + \ln \left\{ \left[\prod_{n=-\infty}^{\infty} \prod_{|\vec{p}| < \Lambda} V \int d\Psi_n^\dagger(\vec{p}) d\Psi_n(\vec{p}) \right] \right. \\
&\quad \left. \exp \left[\beta V \sum_{n=-\infty}^{\infty} \sum_{|\vec{p}| < \Lambda} \Psi_n^\dagger(\vec{p}) G^{-1}(-i\nu_n, \vec{p}) \Psi_n(\vec{p}) \right] \right\} \\
&= -\beta VU + \sum_{n=-\infty}^{\infty} \sum_{|\vec{p}| < \Lambda} \ln \left\{ V \int d\Psi_n^\dagger(\vec{p}) d\Psi_n(\vec{p}) \right. \\
&\quad \left. \exp \left[\beta V \Psi_n^\dagger(\vec{p}) G^{-1}(-i\nu_n, \vec{p}) \Psi_n(\vec{p}) \right] \right\} \\
&= -\beta VU + \sum_{|\vec{p}| < \Lambda} \sum_{n=-\infty}^{\infty} \ln[\beta^4 \det G^{-1}(-i\nu_n, \vec{p})].
\end{aligned} \tag{A.6}$$

Since

$$\det G^{-1}(\omega, \vec{p}) = \prod_{i=1}^4 [\omega - \omega_i(\vec{p})], \tag{A.7}$$

we have

$$\begin{aligned}
\ln \mathcal{Z} &= -\beta VU + \sum_{|\vec{p}| < \Lambda} \sum_{n=-\infty}^{\infty} \ln \left\{ \beta^4 \prod_{i=1}^4 [-i\nu_n - \omega_i(\vec{p})] \right\} \\
&= -\beta VU + \frac{1}{2} \sum_{|\vec{p}| < \Lambda} \sum_{i=1}^4 \sum_{n=-\infty}^{\infty} \ln[(2n + 1)^2 \pi^2 + \beta^2 \omega_i^2(\vec{p})] \\
&= -\beta VU + \frac{1}{2} \sum_{|\vec{p}| < \Lambda} \sum_{i=1}^4 \sum_{n=-\infty}^{\infty} \int^{\beta^2 \omega_i^2(\vec{p})} \frac{d\theta^2}{(2n + 1)^2 \pi^2 + \theta^2} \\
&= -\beta VU + \frac{1}{2} \sum_{|\vec{p}| < \Lambda} \sum_{i=1}^4 \int^{\beta^2 \omega_i^2(\vec{p})} \frac{d\theta^2}{\theta} \left(\frac{1}{2} - \frac{1}{e^\theta + 1} \right) \\
&= -\beta VU + \sum_{|\vec{p}| < \Lambda} \sum_{i=1}^4 \left\{ \frac{1}{2} \beta |\omega_i(\vec{p})| + \ln \left[1 + e^{-\beta |\omega_i(\vec{p})|} \right] \right\},
\end{aligned} \tag{A.8}$$

where we have dropped β -independent terms and used the following summation formula:

$$\sum_{n=-\infty}^{\infty} \frac{1}{(n - x)(n - y)} = \frac{\pi(\cot \pi x - \cot \pi y)}{y - x}. \tag{A.9}$$

Then, the thermodynamic potential is given by

$$\begin{aligned}
\Omega &= -\frac{\ln \mathcal{Z}}{\beta V} = U + \frac{1}{V} \sum_{|\vec{p}| < \Lambda} \sum_{i=1}^4 \left\{ -\frac{1}{2} |\omega_i(\vec{p})| - \frac{1}{\beta} \ln \left[1 + e^{-\beta |\omega_i(\vec{p})|} \right] \right\} \\
&= U - \frac{1}{4\pi^2} \int_0^\Lambda dp p^2 \sum_{i=1}^4 |\omega_i(p)| - \frac{1}{2\pi^2 \beta} \int_0^\Lambda dp p^2 \sum_{i=1}^4 \ln \left[1 + e^{-\beta |\omega_i(p)|} \right],
\end{aligned} \tag{A.10}$$

which is just a collection of fermionic harmonic oscillators [85].

The thermodynamic potential at zero temperature is given by

$$\begin{aligned}\Omega = & U + f(0, \sqrt{\max(0, \min(B_+, \Lambda^2))}, A_-, \Delta_+) \\ & + f(\sqrt{\min(\Lambda^2, \max(B_+, 0))}, \Lambda, A_+, 0) \\ & + f(0, \sqrt{\max(0, \min(B_-, \Lambda^2))}, A_-, \Delta_-) \\ & + f(\sqrt{\min(\Lambda^2, \max(B_-, 0))}, \Lambda, A_+, 0),\end{aligned}\tag{A.11}$$

where

$$\Delta_{\pm} := \sqrt{|\Delta_s|^2 + |\Delta_v|^2 \pm 2|\Delta_s||\Delta_v|\cos\theta},\tag{A.12}$$

$$A_{\pm} := 2m(-\mu + M \pm \lambda),\tag{A.13}$$

$$B_{\pm} := 2m\left(\frac{\Delta_{\pm}^2}{\lambda} + \mu - M\right),\tag{A.14}$$

$$\begin{aligned}f(p_1, p_2, A, \Delta) := & -\frac{1}{8\pi^2 m} \int_{p_1}^{p_2} dp p^2 \sqrt{(p^2 + A)^2 + (4m\Delta)^2} \\ = & \frac{p_1^3}{600\pi^2 m} \left[15\sqrt{(A + p_1^2)^2 + (4m\Delta)^2} \right. \\ & + 6\sqrt{\frac{A^2 p_1^4}{A^2 + (4m\Delta)^2}} F_1\left(\frac{5}{2}; \frac{1}{2}, \frac{1}{2}, \frac{7}{2}; -\frac{p_1^2}{A+4im\Delta}, -\frac{p_1^2}{A-4im\Delta}\right) \\ & + 10\sqrt{A^2 + (4m\Delta)^2} F_1\left(\frac{3}{2}; \frac{1}{2}, \frac{1}{2}, \frac{5}{2}; -\frac{p_1^2}{A+4im\Delta}, -\frac{p_1^2}{A-4im\Delta}\right) \Big] \\ & - \frac{p_2^3}{600\pi^2 m} \left[15\sqrt{(A + p_2^2)^2 + (4m\Delta)^2} \right. \\ & + 6\sqrt{\frac{A^2 p_2^4}{A^2 + (4m\Delta)^2}} F_1\left(\frac{5}{2}; \frac{1}{2}, \frac{1}{2}, \frac{7}{2}; -\frac{p_2^2}{A+4im\Delta}, -\frac{p_2^2}{A-4im\Delta}\right) \\ & + 10\sqrt{A^2 + (4m\Delta)^2} F_1\left(\frac{3}{2}; \frac{1}{2}, \frac{1}{2}, \frac{5}{2}; -\frac{p_2^2}{A+4im\Delta}, -\frac{p_2^2}{A-4im\Delta}\right) \Big],\end{aligned}\tag{A.15}$$

and F_1 is the Appell hypergeometric function.

B Numerical calculation of the non-relativistic mean field model

Figure 6 shows the result of the numerical minimization of Ω with $g'_s > g'_v$ (see the blue region in figure 2b). When the temperature is low and the heavy-light coupling is strong, $|\Delta_s| \neq 0$, but $M = |\Delta_v| = 0$ (see figure 6a), so that our model is reduced to a lattice version of the Anderson model as follows:

$$\mathcal{L}_{\text{MF}} \rightarrow \psi^\dagger \left(i \frac{\partial}{\partial t} + \frac{\nabla^2}{2m} + \mu \right) \psi + \chi^\dagger \left(i \frac{\partial}{\partial t} - \lambda \right) \chi + |\Delta_s|(\psi^\dagger \chi + \chi^\dagger \psi) - \frac{|\Delta_s|^2}{g'_s}.\tag{B.1}$$

Unlike the mean field theory of superconductivity, where the existence of the condensation is determined only by whether coupling is turned on or off [86], in our case, a phase transition occurs at some critical coupling. When $\lambda = 0$, the phase transition is second-order (see the blue lines in figures 6e and 6i). However, when $\lambda \neq 0$, the phase transition

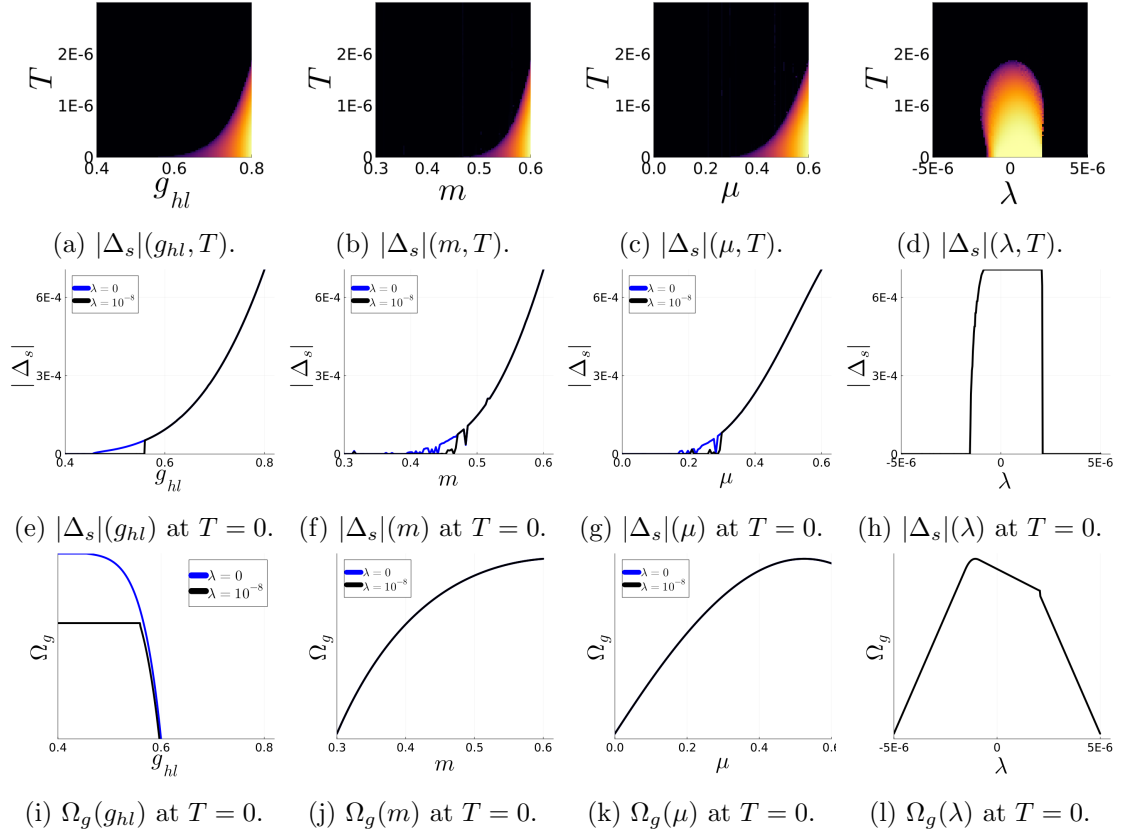


Figure 6: Numerical minimization of the thermodynamic potential. $g_t = 0.01$, $g_{hl} := g'_s/2 = g'_v$. $\lambda = 0$ for the blue lines. (a,e,i) $m = \mu = 0.6$, $\lambda = 10^{-8}$. (b,f,j) $g_{hl} = 0.8$, $\mu = 0.6$, $\lambda = 10^{-8}$. (c,g,k) $g_{hl} = 0.8$, $m = 0.6$, $\lambda = 10^{-8}$. (d,i,l) $g_{hl} = 0.8$, $m = \mu = 0.6$. (a,b,c,d) show the phase diagrams. The brighter it is, the higher the value of $|\Delta_s|$. (e,f,g,h) show the gap equations and (i,j,k,l) show the thermodynamic potential Ω_g of the ground state at $T = 0$ versus g_{hl} , m , μ , and λ . M and $|\Delta_v|$ do not appear in this numerical calculation.

is first-order (see figure 3a and the black lines in figure 6e and 6i). For first-order quantum phase transition to occur, the system must have a scale [87]; in our case, it is λ . As we decrease m or μ , $|\Delta_s|$ disappears (see figure 6f and 6g). Also, as we increase the magnitude of λ , Δ_s becomes zero (see figure 6h).

C Details of the holographic Kondo lattice model

C.1 Probe spinor fields in the bulk

Define

$$\rho_k^S := \begin{pmatrix} \phi_{k,1}^{(1)} \\ \phi_{k,2}^{(1)} \\ \phi_{k,1}^{(2)} \\ \phi_{k,2}^{(2)} \end{pmatrix}, \quad \rho_k^C := \begin{pmatrix} \phi_{k,3}^{(1)} \\ \phi_{k,4}^{(1)} \\ \phi_{k,3}^{(2)} \\ \phi_{k,4}^{(2)} \end{pmatrix}, \quad \varrho_k^S := \begin{pmatrix} A_k^{(1)} \\ A_k^{(2)} \end{pmatrix}, \quad \varrho_k^C := \begin{pmatrix} D_k^{(1)} \\ D_k^{(2)} \end{pmatrix} \quad (\text{C.1})$$

such that

$$\rho_k^S \approx \begin{pmatrix} A_k^{(1)} u^{m_1} \\ A_k^{(2)} u^{m_2} \end{pmatrix} = \begin{pmatrix} u^{m_1} & 0 & 0 & 0 \\ 0 & u^{m_1} & 0 & 0 \\ 0 & 0 & u^{m_2} & 0 \\ 0 & 0 & 0 & u^{m_2} \end{pmatrix} \varrho_k^S, \quad (\text{C.2})$$

$$\rho_k^C \approx \begin{pmatrix} D_k^{(1)} u^{-m_1} \\ D_k^{(2)} u^{-m_2} \end{pmatrix} = \begin{pmatrix} u^{-m_1} & 0 & 0 & 0 \\ 0 & u^{-m_1} & 0 & 0 \\ 0 & 0 & u^{-m_2} & 0 \\ 0 & 0 & 0 & u^{-m_2} \end{pmatrix} \varrho_k^C \quad (\text{C.3})$$

near the boundary. Then, the equations of motion of the probe spinor fields read

$$\partial_u \rho_k^S = \mathcal{D}_k^{SS} \rho_k^S + \mathcal{D}_k^{SC} \rho_k^C, \quad \partial_u \rho_k^C = \mathcal{D}_k^{CS} \rho_k^S + \mathcal{D}_k^{CC} \rho_k^C, \quad (\text{C.4})$$

where

$$\mathcal{D}_k^{SS} := \begin{pmatrix} \frac{m_1 \sigma_0}{u\sqrt{f}} & -\frac{V\Phi_s \sigma_0}{u\sqrt{f}} \\ -\frac{V\Phi_s \sigma_0}{u\sqrt{f}} & \frac{(m_2 - g_2 \Phi_s) \sigma_0}{u\sqrt{f}} \end{pmatrix}, \quad (\text{C.5})$$

$$\mathcal{D}_k^{SC} := \begin{pmatrix} -\frac{(\omega + q_1 A_t) \sigma_2}{f\sqrt{\chi}} - \frac{ik_x \sigma_1 + ik_y \sigma_3}{\sqrt{f}} + \frac{g_1 \Phi_{ps} \sigma_0}{u\sqrt{f}} & 0 \\ 0 & -\frac{(\omega + q_2 A_t) \sigma_2}{f\sqrt{\chi}} - \frac{ik_x \sigma_1 + ik_y \sigma_3}{\sqrt{f}} \end{pmatrix}, \quad (\text{C.6})$$

$$\mathcal{D}_k^{CS} := \begin{pmatrix} \frac{(\omega + q_1 A_t) \sigma_2}{f\sqrt{\chi}} + \frac{ik_x \sigma_1 + ik_y \sigma_3}{\sqrt{f}} + \frac{g_1 \Phi_{ps} \sigma_0}{u\sqrt{f}} & 0 \\ 0 & \frac{(\omega + q_2 A_t) \sigma_2}{f\sqrt{\chi}} + \frac{ik_x \sigma_1 + ik_y \sigma_3}{\sqrt{f}} \end{pmatrix}, \quad (\text{C.7})$$

$$\mathcal{D}_k^{CC} := \begin{pmatrix} -\frac{m_1 \sigma_0}{u\sqrt{f}} & \frac{V\Phi_s \sigma_0}{u\sqrt{f}} \\ \frac{V\Phi_s \sigma_0}{u\sqrt{f}} & -\frac{(m_2 - g_2 \Phi_s) \sigma_0}{u\sqrt{f}} \end{pmatrix}. \quad (\text{C.8})$$

For the standard-standard quantization $\Gamma^{(1)} = \Gamma^{(2)} = i\mathbb{I}_4$, we can choose

$$Q^{(1)} = Q^{(2)} = \begin{pmatrix} 0 & \sigma_1 \end{pmatrix}, \quad P^{(1)} = P^{(2)} = \begin{pmatrix} -i\sigma_3 & 0 \end{pmatrix}. \quad (\text{C.9})$$

Then,

$$C_k = \begin{pmatrix} Q^{(1)} \varphi_k^{(1)} \\ Q^{(2)} \varphi_k^{(2)} \end{pmatrix} = \begin{pmatrix} \sigma_1 D_k^{(1)} \\ \sigma_1 D_k^{(2)} \end{pmatrix} = \begin{pmatrix} \sigma_1 & 0 \\ 0 & \sigma_1 \end{pmatrix} \varrho_k^C, \quad (\text{C.10})$$

$$J_k = \begin{pmatrix} P^{(1)} \varphi_k^{(1)} \\ P^{(2)} \varphi_k^{(2)} \end{pmatrix} = \begin{pmatrix} -i\sigma_3 A_k^{(1)} \\ -i\sigma_3 A_k^{(2)} \end{pmatrix} = \begin{pmatrix} -i\sigma_3 & 0 \\ 0 & -i\sigma_3 \end{pmatrix} \varrho_k^S; \quad (\text{C.11})$$

$$\therefore \varrho_k^C = \begin{pmatrix} \sigma_1 & 0 \\ 0 & \sigma_1 \end{pmatrix}^{-1} G_k \begin{pmatrix} -i\sigma_3 & 0 \\ 0 & -i\sigma_3 \end{pmatrix} \varrho_k^S \quad (\forall \varrho_k^S \in \mathbb{C}^4). \quad (\text{C.12})$$

Correspondingly, define

$$\rho_k^C \equiv \begin{pmatrix} \sigma_1 & 0 \\ 0 & \sigma_1 \end{pmatrix}^{-1} \mathcal{G}_k \begin{pmatrix} -i\sigma_3 & 0 \\ 0 & -i\sigma_3 \end{pmatrix} \rho_k^S, \quad \tilde{\mathcal{G}}_k := \begin{pmatrix} \sigma_1 & 0 \\ 0 & \sigma_1 \end{pmatrix}^{-1} \mathcal{G}_k \begin{pmatrix} -i\sigma_3 & 0 \\ 0 & -i\sigma_3 \end{pmatrix} \quad (\text{C.13})$$

such that

$$G_k = \lim_{u \rightarrow 0} \begin{pmatrix} u^{2m_1} & 0 & 0 & 0 \\ 0 & u^{2m_1} & 0 & 0 \\ 0 & 0 & u^{2m_2} & 0 \\ 0 & 0 & 0 & u^{2m_2} \end{pmatrix} \mathcal{G}_k. \quad (\text{C.14})$$

From the equations of motion of the probe spinor fields and arbitrariness of ϱ_k^S , we can obtain the flow equations as follows (see ref. [81]):

$$\partial_u \rho_k^C = (\partial_u \tilde{\mathcal{G}}_k) \rho_k^S + \tilde{\mathcal{G}}_k (\partial_u \rho_k^S) \quad (\text{C.15})$$

$$\Rightarrow \mathcal{D}_k^{CS} \rho_k^C + \mathcal{D}_k^{CC} \rho_k^C = (\partial_u \tilde{\mathcal{G}}_k) \rho_k^S + \tilde{\mathcal{G}}_k (\mathcal{D}_k^{SS} \rho_k^S + \mathcal{D}_k^{SC} \rho_k^C) \quad (\text{C.16})$$

$$\Rightarrow (\mathcal{D}_k^{CC} - \tilde{\mathcal{G}}_k \mathcal{D}_k^{SC}) \tilde{\mathcal{G}}_k \rho_k^S = (\partial_u \tilde{\mathcal{G}}_k + \tilde{\mathcal{G}}_k \mathcal{D}_k^{SS} - \mathcal{D}_k^{CS}) \rho_k^S; \quad (\text{C.17})$$

$$\therefore \partial_u \tilde{\mathcal{G}}_k = \mathcal{D}_k^{CS} + \mathcal{D}_k^{CC} \tilde{\mathcal{G}}_k - \tilde{\mathcal{G}}_k \mathcal{D}_k^{SS} - \tilde{\mathcal{G}}_k \mathcal{D}_k^{SC} \tilde{\mathcal{G}}_k, \quad (\text{C.18})$$

or equivalently,

$$\partial_u \mathcal{G}_k = \tilde{\mathcal{D}}_k^1 + \tilde{\mathcal{D}}_k^2 \mathcal{G}_k - \mathcal{G}_k \tilde{\mathcal{D}}_k^3 - \mathcal{G}_k \tilde{\mathcal{D}}_k^4 \mathcal{G}_k, \quad (\text{C.19})$$

where

$$\begin{aligned} \tilde{\mathcal{D}}_k^1 &:= \begin{pmatrix} \sigma_1 & 0 \\ 0 & \sigma_1 \end{pmatrix} \mathcal{D}_k^{CS} \begin{pmatrix} -i\sigma_3 & 0 \\ 0 & -i\sigma_3 \end{pmatrix}^{-1} \\ &= \begin{pmatrix} -\frac{(\omega+q_1 A_t)\sigma_0}{f\sqrt{\chi}} - \frac{k_x \sigma_3 + k_y \sigma_1}{\sqrt{f}} + \frac{g_1 \Phi_{ps} \sigma_2}{u\sqrt{f}} & 0 \\ 0 & -\frac{(\omega+q_2 A_t)\sigma_0}{f\sqrt{\chi}} - \frac{k_x \sigma_3 + k_y \sigma_1}{\sqrt{f}} \end{pmatrix}, \end{aligned} \quad (\text{C.20})$$

$$\tilde{\mathcal{D}}_k^2 := \begin{pmatrix} \sigma_1 & 0 \\ 0 & \sigma_1 \end{pmatrix} \mathcal{D}_k^{CC} \begin{pmatrix} \sigma_1 & 0 \\ 0 & \sigma_1 \end{pmatrix}^{-1} = \begin{pmatrix} -\frac{m_1 \sigma_0}{u\sqrt{f}} & \frac{V \Phi_s \sigma_0}{u\sqrt{f}} \\ \frac{V \Phi_s \sigma_0}{u\sqrt{f}} & -\frac{(m_2 - g_2 \Phi_s) \sigma_0}{u\sqrt{f}} \end{pmatrix}, \quad (\text{C.21})$$

$$\tilde{\mathcal{D}}_k^3 := \begin{pmatrix} -i\sigma_3 & 0 \\ 0 & -i\sigma_3 \end{pmatrix} \mathcal{D}_k^{SS} \begin{pmatrix} -i\sigma_3 & 0 \\ 0 & -i\sigma_3 \end{pmatrix}^{-1} = \begin{pmatrix} \frac{m_1 \sigma_0}{u\sqrt{f}} & -\frac{V \Phi_s \sigma_0}{u\sqrt{f}} \\ -\frac{V \Phi_s \sigma_0}{u\sqrt{f}} & \frac{(m_2 - g_2 \Phi_s) \sigma_0}{u\sqrt{f}} \end{pmatrix}, \quad (\text{C.22})$$

$$\begin{aligned} \tilde{\mathcal{D}}_k^4 &:= \begin{pmatrix} -i\sigma_3 & 0 \\ 0 & -i\sigma_3 \end{pmatrix} \mathcal{D}_k^{SC} \begin{pmatrix} \sigma_1 & 0 \\ 0 & \sigma_1 \end{pmatrix}^{-1} \\ &= \begin{pmatrix} \frac{(\omega+q_1 A_t)\sigma_0}{f\sqrt{\chi}} - \frac{k_x \sigma_3 + k_y \sigma_1}{\sqrt{f}} + \frac{g_1 \Phi_{ps} \sigma_2}{u\sqrt{f}} & 0 \\ 0 & \frac{(\omega+q_2 A_t)\sigma_0}{f\sqrt{\chi}} - \frac{k_x \sigma_3 + k_y \sigma_1}{\sqrt{f}} \end{pmatrix}. \end{aligned} \quad (\text{C.23})$$

C.2 Probe spinor fields near the horizon

The asymptotic behavior of the probe spinor fields near the horizon is as follows:

$$\phi_k^{(j)} \approx \underbrace{\left(1 - \frac{u}{u_h}\right)^{-\frac{i\omega}{|f'_h|\sqrt{\chi}h}} \begin{pmatrix} a_k^{(j)} \\ b_k^{(j)} \\ -b_k^{(j)} \\ a_k^{(j)} \end{pmatrix}}_{\text{infalling}} + \underbrace{\left(1 - \frac{u}{u_h}\right)^{\frac{i\omega}{|f'_h|\sqrt{\chi}h}} \begin{pmatrix} c_k^{(j)} \\ d_k^{(j)} \\ d_k^{(j)} \\ -c_k^{(j)} \end{pmatrix}}_{\text{outgoing}}, \quad (\text{C.24})$$

where $f'_h := f'(u_h)$, $\chi_h := \chi(u_h)$, and $a_k^{(j)}, b_k^{(j)}, c_k^{(j)}, d_k^{(j)}$ are expansion coefficients. Imposing the infalling boundary condition $c_k^{(j)} = d_k^{(j)} = 0$, we have

$$\rho_k^S \approx \left(1 - \frac{u}{u_h}\right)^{-\frac{i\omega}{|f'_h|\sqrt{\chi_h}}} \begin{pmatrix} a_k^{(1)} \\ b_k^{(1)} \\ a_k^{(2)} \\ b_k^{(2)} \end{pmatrix}, \quad \rho_k^C \approx \left(1 - \frac{u}{u_h}\right)^{-\frac{i\omega}{|f'_h|\sqrt{\chi_h}}} \begin{pmatrix} -b_k^{(1)} \\ a_k^{(1)} \\ -b_k^{(2)} \\ a_k^{(2)} \end{pmatrix}. \quad (\text{C.25})$$

Therefore, the infalling boundary condition gives

$$\begin{pmatrix} -b_k^{(1)} \\ a_k^{(1)} \\ -b_k^{(2)} \\ a_k^{(2)} \end{pmatrix} = \begin{pmatrix} \sigma_1 & 0 \\ 0 & \sigma_1 \end{pmatrix}^{-1} \mathcal{G}_k(u_h) \begin{pmatrix} -i\sigma_3 & 0 \\ 0 & -i\sigma_3 \end{pmatrix} \begin{pmatrix} a_k^{(1)} \\ b_k^{(1)} \\ a_k^{(2)} \\ b_k^{(2)} \end{pmatrix} \Rightarrow \mathcal{G}_k(u_h) = i\mathbb{I}_4, \quad (\text{C.26})$$

where we have used arbitrariness of $a_k^{(j)}, b_k^{(j)}$.

C.3 From standard-standard to standard-mixed quantization

Suppose we know the Green's function G_k^{SS} in the standard-standard quantization $\Gamma^{(1)} = \Gamma^{(2)} = i\mathbb{I}_4$ (to see how to get G_k^{SS} , see appendix C). When we consider the standard-mixed quantization $\Gamma^{(1)} = i\mathbb{I}_4, \Gamma^{(2)} = \Gamma^{\text{XY}}$, we can choose

$$P^{(1)} = \begin{pmatrix} -i & 0 & 0 & 0 \\ 0 & i & 0 & 0 \end{pmatrix}, \quad Q^{(1)} = \begin{pmatrix} 0 & 0 & 0 & 1 \\ 0 & 0 & 1 & 0 \end{pmatrix}, \quad (\text{C.27})$$

$$P^{(2)} = \frac{1}{\sqrt{2}} \begin{pmatrix} -i & 1 & 0 & 0 \\ 0 & 0 & i & 1 \end{pmatrix}, \quad Q^{(2)} = \frac{1}{\sqrt{2}} \begin{pmatrix} 0 & 0 & -i & 1 \\ i & 1 & 0 & 0 \end{pmatrix}. \quad (\text{C.28})$$

Substituting

$$\begin{aligned} \varrho_k^C &= \begin{pmatrix} \sigma_1 & 0 \\ 0 & \sigma_1 \end{pmatrix}^{-1} G_k^{\text{SS}} \begin{pmatrix} -i\sigma_3 & 0 \\ 0 & -i\sigma_3 \end{pmatrix} \varrho_k^S \\ &\Leftrightarrow \begin{pmatrix} D_k^{(1)} \\ D_k^{(2)} \end{pmatrix} = -i \begin{pmatrix} \sigma_1 & 0 \\ 0 & \sigma_1 \end{pmatrix} G_k^{\text{SS}} \begin{pmatrix} \sigma_3 & 0 \\ 0 & \sigma_3 \end{pmatrix} \begin{pmatrix} A_k^{(1)} \\ A_k^{(2)} \end{pmatrix} \end{aligned} \quad (\text{C.29})$$

to

$$\begin{aligned} C_k &= G_k^{\text{SM}} J_k \Leftrightarrow \begin{pmatrix} Q^{(1)} \varphi_k^{(1)} \\ Q^{(2)} \varphi_k^{(2)} \end{pmatrix} = G_k^{\text{SM}} \begin{pmatrix} P^{(1)} \varphi_k^{(1)} \\ P^{(2)} \varphi_k^{(2)} \end{pmatrix} \\ &\Leftrightarrow \begin{pmatrix} Q^{(1)} \begin{pmatrix} A_k^{(1)} \\ D_k^{(1)} \end{pmatrix} \\ Q^{(2)} \begin{pmatrix} A_k^{(2)} \\ D_k^{(2)} \end{pmatrix} \end{pmatrix} = G_k^{\text{SM}} \begin{pmatrix} P^{(1)} \begin{pmatrix} A_k^{(1)} \\ D_k^{(1)} \end{pmatrix} \\ P^{(2)} \begin{pmatrix} A_k^{(2)} \\ D_k^{(2)} \end{pmatrix} \end{pmatrix}, \end{aligned} \quad (\text{C.30})$$

we obtain

$$\begin{pmatrix} Q^{(1)} \begin{pmatrix} A_k^{(1)} \\ -i(\sigma_1 \ 0) G_k^{\text{SS}} \begin{pmatrix} \sigma_3 & 0 \\ 0 & \sigma_3 \end{pmatrix} A_k^{(1)} \end{pmatrix} \\ Q^{(2)} \begin{pmatrix} A_k^{(2)} \\ -i(0 \ \sigma_1) G_k^{\text{SS}} \begin{pmatrix} \sigma_3 & 0 \\ 0 & \sigma_3 \end{pmatrix} A_k^{(2)} \end{pmatrix} \end{pmatrix} = G_k^{\text{SM}} \begin{pmatrix} P^{(1)} \begin{pmatrix} A_k^{(1)} \\ -i(\sigma_1 \ 0) G_k^{\text{SS}} \begin{pmatrix} \sigma_3 & 0 \\ 0 & \sigma_3 \end{pmatrix} A_k^{(1)} \end{pmatrix} \\ P^{(2)} \begin{pmatrix} A_k^{(2)} \\ -i(0 \ \sigma_1) G_k^{\text{SS}} \begin{pmatrix} \sigma_3 & 0 \\ 0 & \sigma_3 \end{pmatrix} A_k^{(2)} \end{pmatrix} \end{pmatrix}; \quad (\text{C.31})$$

$$\therefore G_k^{\text{SM}} = \begin{pmatrix} Q^{(1)} \begin{pmatrix} (\sigma_0 \ 0) \\ -i(\sigma_1 \ 0) G_k^{\text{SS}} \begin{pmatrix} \sigma_3 & 0 \\ 0 & \sigma_3 \end{pmatrix} \end{pmatrix} \\ Q^{(2)} \begin{pmatrix} (0 \ \sigma_0) \\ -i(0 \ \sigma_1) G_k^{\text{SS}} \begin{pmatrix} \sigma_3 & 0 \\ 0 & \sigma_3 \end{pmatrix} \end{pmatrix} \end{pmatrix} \begin{pmatrix} P^{(1)} \begin{pmatrix} (\sigma_0 \ 0) \\ -i(\sigma_1 \ 0) G_k^{\text{SS}} \begin{pmatrix} \sigma_3 & 0 \\ 0 & \sigma_3 \end{pmatrix} \end{pmatrix} \\ P^{(2)} \begin{pmatrix} (0 \ \sigma_0) \\ -i(0 \ \sigma_1) G_k^{\text{SS}} \begin{pmatrix} \sigma_3 & 0 \\ 0 & \sigma_3 \end{pmatrix} \end{pmatrix} \end{pmatrix}^{-1}, \quad (\text{C.32})$$

where we have used arbitrariness of $A_k^{(j)}$. The trace of the Green's function G_k^{SM} in the standard-mixed quantization is then given by

$$\begin{aligned} \text{tr } G_k^{\text{SM}} &= (G_{k,11}^{\text{SS}} + G_{k,22}^{\text{SS}}) + \frac{2(G_{k,33}^{\text{SS}} G_{k,44}^{\text{SS}} - G_{k,34}^{\text{SS}} G_{k,43}^{\text{SS}} - 1)}{G_{k,33}^{\text{SS}} - iG_{k,34}^{\text{SS}} + iG_{k,43}^{\text{SS}} + G_{k,44}^{\text{SS}}} \\ &\quad + \frac{(-G_{k,13}^{\text{SS}} + iG_{k,14}^{\text{SS}})(G_{k,31}^{\text{SS}} + iG_{k,41}^{\text{SS}})}{G_{k,33}^{\text{SS}} - iG_{k,34}^{\text{SS}} + iG_{k,43}^{\text{SS}} + G_{k,44}^{\text{SS}}} \\ &\quad + \frac{(-G_{k,23}^{\text{SS}} + iG_{k,24}^{\text{SS}})(G_{k,32}^{\text{SS}} + iG_{k,42}^{\text{SS}})}{G_{k,33}^{\text{SS}} - iG_{k,34}^{\text{SS}} + iG_{k,43}^{\text{SS}} + G_{k,44}^{\text{SS}}}. \end{aligned} \quad (\text{C.33})$$

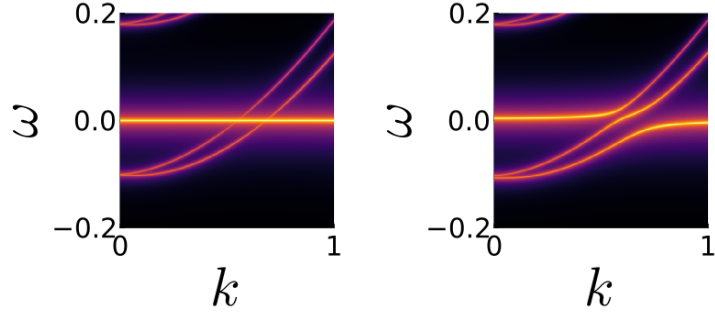
The explicit form of the above translation formula (C.33) and the components of Green's function depend on the choice of the spinor representation. However, their representation dependencies cancel each other, so the trace of Green's function is invariant under a change of spinor representation. The method in this subsection can be applied to other quantizations.

D Trial holographic models for the Kondo lattice

D.1 With $g_1 \Phi_{\text{ps}} \cdot i\mathbb{I}_4$ rather than $g_1 \Phi_{\text{ps}} \cdot \Gamma^5$

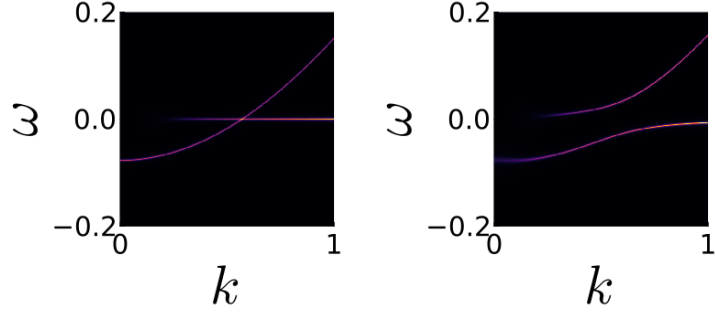
When we set

$$\begin{aligned} S_{\text{spin}} &= S_{\text{spin, bdy}} + \sum_{j=1}^2 \int d^4x \sqrt{-g} i \bar{\psi}^{(j)} \left[\frac{1}{2} \left(\vec{D}^{(j)} - \overleftarrow{D}^{(j)} \right) - m_j \right] \psi^{(j)} \\ &\quad + \int d^4x \sqrt{-g} \begin{pmatrix} \bar{\psi}^{(1)} \\ \bar{\psi}^{(2)} \end{pmatrix}^T \begin{pmatrix} g_1 \Phi_{\text{ps}} \cdot i\mathbb{I}_4 & V \Phi_{\text{s}} \cdot i\mathbb{I}_4 \\ V \Phi_{\text{s}} \cdot i\mathbb{I}_4 & g_2 \Phi_{\text{s}} \cdot i\mathbb{I}_4 \end{pmatrix} \begin{pmatrix} \psi^{(1)} \\ \psi^{(2)} \end{pmatrix}, \end{aligned} \quad (\text{D.1})$$



(a) $A(\omega, k), V = 0, u_h = 10$. (b) $A(\omega, k), V = 0.5, u_h = 10$.

Figure 7: Spectral function with scalar type interaction. The parameters except $g_1 = 8.2$ are same with figure 5.



(a) $A(\omega, k), V = 0, u_h = 10$. (b) $A(\omega, k), V = 0.5, u_h = 10$.

Figure 8: Spectral function without band isolation. The parameters except $g_2 = 0$ are same with figure 5.

instead of eq. (3.3), eqs. (C.20), (C.21), (C.22), and (C.23) are replaced by

$$\tilde{\mathcal{D}}_k^1 = \begin{pmatrix} -\frac{(\omega+q_1 A_t)\sigma_0}{f\sqrt{\chi}} - \frac{k_x\sigma_3+k_y\sigma_1}{\sqrt{f}} & 0 \\ 0 & -\frac{(\omega+q_2 A_t)\sigma_0}{f\sqrt{\chi}} - \frac{k_x\sigma_3+k_y\sigma_1}{\sqrt{f}} \end{pmatrix}, \quad (\text{D.2})$$

$$\tilde{\mathcal{D}}_k^2 = \begin{pmatrix} -\frac{(m_1-g_1\Phi_{\text{ps}})\sigma_0}{u\sqrt{f}} & \frac{V\Phi_s\sigma_0}{u\sqrt{f}} \\ \frac{V\Phi_s\sigma_0}{u\sqrt{f}} & -\frac{(m_2-g_2\Phi_s)\sigma_0}{u\sqrt{f}} \end{pmatrix}, \quad (\text{D.3})$$

$$\tilde{\mathcal{D}}_k^3 = \begin{pmatrix} \frac{(m_1-g_1\Phi_{\text{ps}})\sigma_0}{u\sqrt{f}} & -\frac{V\Phi_s\sigma_0}{u\sqrt{f}} \\ -\frac{V\Phi_s\sigma_0}{u\sqrt{f}} & \frac{(m_2-g_2\Phi_s)\sigma_0}{u\sqrt{f}} \end{pmatrix}, \quad (\text{D.4})$$

$$\tilde{\mathcal{D}}_k^4 = \begin{pmatrix} \frac{(\omega+q_1 A_t)\sigma_0}{f\sqrt{\chi}} - \frac{k_x\sigma_3+k_y\sigma_1}{\sqrt{f}} & 0 \\ 0 & \frac{(\omega+q_2 A_t)\sigma_0}{f\sqrt{\chi}} - \frac{k_x\sigma_3+k_y\sigma_1}{\sqrt{f}} \end{pmatrix}, \quad (\text{D.5})$$

and the hybridization does not open gap completely (see figure 7).

D.2 Without $g_2\Phi_s \cdot i\mathbb{I}_4$

When we set

$$\begin{aligned}
S_{\text{spin}} = S_{\text{spin, bdy}} + \sum_{j=1}^2 \int d^4x \sqrt{-g} i \bar{\psi}^{(j)} \left[\frac{1}{2} \left(\overrightarrow{\not{D}}^{(j)} - \overleftarrow{\not{D}}^{(j)} \right) - m_j \right] \psi^{(j)} \\
+ \int d^4x \sqrt{-g} \begin{pmatrix} \bar{\psi}^{(1)} \\ \bar{\psi}^{(2)} \end{pmatrix}^T \begin{pmatrix} g_1 \Phi_{\text{ps}} \cdot \Gamma^5 & V \Phi_s \cdot i\mathbb{I}_4 \\ V \Phi_s \cdot i\mathbb{I}_4 & 0 \end{pmatrix} \begin{pmatrix} \psi^{(1)} \\ \psi^{(2)} \end{pmatrix},
\end{aligned} \tag{D.6}$$

instead of eq. (3.3), the flat band is dim near $\vec{k} = 0$ (see figure 8).

References

- [1] W. Meissner and B. Voigt, *Messungen mit hilfe von flüssigem helium xi widerstand der reinen metalle in tiefen temperaturen*, *Annalen der Physik* **399** (1930) 761
[<https://onlinelibrary.wiley.com/doi/pdf/10.1002/andp.19303990702>].
- [2] P.W. Anderson, *Localized magnetic states in metals*, *Phys. Rev.* **124** (1961) 41.
- [3] C. Zener, *Interaction between the d shells in the transition metals*, *Phys. Rev.* **81** (1951) 440.
- [4] M.A. Ruderman and C. Kittel, *Indirect exchange coupling of nuclear magnetic moments by conduction electrons*, *Phys. Rev.* **96** (1954) 99.
- [5] T. Kasuya, *A Theory of Metallic Ferro- and Antiferromagnetism on Zener's Model*, *Progress of Theoretical Physics* **16** (1956) 45
[<https://academic.oup.com/ptp/article-pdf/16/1/45/5266722/16-1-45.pdf>].
- [6] K. Yosida, *Magnetic properties of cu-mn alloys*, *Phys. Rev.* **106** (1957) 893.
- [7] K. Yosida, *Anomalous electrical resistivity and magnetoresistance due to an s - d interaction in cu-mn alloys*, *Phys. Rev.* **107** (1957) 396.
- [8] J. Kondo, *Resistance Minimum in Dilute Magnetic Alloys*, *Progress of Theoretical Physics* **32** (1964) 37
[<https://academic.oup.com/ptp/article-pdf/32/1/37/5193092/32-1-37.pdf>].
- [9] K.G. Wilson and J.B. Kogut, *The renormalization group and the epsilon expansion*, *Phys. Rept.* **12** (1974) 75.
- [10] J.R. Schrieffer and P.A. Wolff, *Relation between the anderson and kondo hamiltonians*, *Phys. Rev.* **149** (1966) 491.
- [11] B. Coqblin and J.R. Schrieffer, *Exchange interaction in alloys with cerium impurities*, *Phys. Rev.* **185** (1969) 847.
- [12] N. Read and D.M. Newns, *On the solution of the coqblin-schrieffer hamiltonian by the large-n expansion technique*, *Journal of Physics C: Solid State Physics* **16** (1983) 3273.
- [13] N. Read and D.M. Newns, *A new functional integral formalism for the degenerate anderson model*, *Journal of Physics C: Solid State Physics* **16** (1983) L1055.
- [14] P. Coleman, $\frac{1}{N}$ expansion for the kondo lattice, *Phys. Rev. B* **28** (1983) 5255.
- [15] P. Coleman, *New approach to the mixed-valence problem*, *Phys. Rev. B* **29** (1984) 3035.

- [16] G. Kotliar and A.E. Ruckenstein, *New functional integral approach to strongly correlated fermi systems: The gutzwiller approximation as a saddle point*, *Phys. Rev. Lett.* **57** (1986) 1362.
- [17] P. Coleman, *Mixed valence as an almost broken symmetry*, *Phys. Rev. B* **35** (1987) 5072.
- [18] A.J. Millis and P.A. Lee, *Large-orbital-degeneracy expansion for the lattice anderson model*, *Phys. Rev. B* **35** (1987) 3394.
- [19] A. Georges and G. Kotliar, *Hubbard model in infinite dimensions*, *Phys. Rev. B* **45** (1992) 6479.
- [20] Z. Fisk, J. Sarrao, S. Cooper, P. Nyhus, G. Boebinger, A. Passner et al., *Kondo insulators*, *Physica B: Condensed Matter* **223-224** (1996) 409.
- [21] H. Tsunetsugu, M. Sigrist and K. Ueda, *The ground-state phase diagram of the one-dimensional kondo lattice model*, *Rev. Mod. Phys.* **69** (1997) 809.
- [22] P.S. Riseborough, *Heavy fermion semiconductors*, *Advances in Physics* **49** (2000) 257 [<https://doi.org/10.1080/000187300243345>].
- [23] M. Dzero, K. Sun, V. Galitski and P. Coleman, *Topological kondo insulators*, *Phys. Rev. Lett.* **104** (2010) 106408.
- [24] P. Coleman, *Heavy fermions and the kondo lattice: a 21st century perspective*, 2015.
- [25] I. Affleck, A.W.W. Ludwig and B.A. Jones, *Conformal-field-theory approach to the two-impurity kondo problem: Comparison with numerical renormalization-group results*, *Phys. Rev. B* **52** (1995) 9528.
- [26] A. Auerbach and K. Levin, *Kondo bosons and the kondo lattice: Microscopic basis for the heavy fermi liquid*, *Phys. Rev. Lett.* **57** (1986) 877.
- [27] H. Im, D.U. Lee, Y. Jo, J. Kim, Y. Chong, W. Song et al., *Observation of kondo condensation in a degenerately doped silicon metal*, *Nature Physics* **19** (2023) 676.
- [28] S. Yasui, K. Suzuki and K. Itakura, *Topology and stability of the kondo phase in quark matter*, *Phys. Rev. D* **96** (2017) 014016.
- [29] K. Suzuki, S. Yasui and K. Itakura, *Interplay between chiral symmetry breaking and the qcd kondo effect*, *Phys. Rev. D* **96** (2017) 114007.
- [30] S. Yasui, K. Suzuki and K. Itakura, *Kondo phase diagram of quark matter*, *Nuclear Physics A* **983** (2019) 90.
- [31] D. Suenaga, K. Suzuki, Y. Araki and S. Yasui, *Kondo effect driven by chirality imbalance*, *Phys. Rev. Res.* **2** (2020) 023312.
- [32] Y. Araki, D. Suenaga, K. Suzuki and S. Yasui, *Two relativistic kondo effects: Classification with particle and antiparticle impurities*, *Phys. Rev. Res.* **3** (2021) 013233.
- [33] T. Ishikawa, K. Nakayama and K. Suzuki, *Kondo effect with wilson fermions*, *Phys. Rev. D* **104** (2021) 094515.
- [34] D. Suenaga, Y. Araki, K. Suzuki and S. Yasui, *Heavy-quark spin polarization induced by the kondo effect in a magnetic field*, *Phys. Rev. D* **105** (2022) 074028.
- [35] K. Hattori, D. Suenaga, K. Suzuki and S. Yasui, *Dirac kondo effect under magnetic catalysis*, *Phys. Rev. B* **108** (2023) 245110.

- [36] Y. Nambu and G. Jona-Lasinio, *Dynamical model of elementary particles based on an analogy with superconductivity. i*, *Phys. Rev.* **122** (1961) 345.
- [37] Y. Nambu and G. Jona-Lasinio, *Dynamical model of elementary particles based on an analogy with superconductivity. ii*, *Phys. Rev.* **124** (1961) 246.
- [38] J. Maldacena, *The large- n limit of superconformal field theories and supergravity*, *International Journal of Theoretical Physics* **38** (1999) 1113.
- [39] E. Witten, *Anti-de Sitter space and holography*, *Adv. Theor. Math. Phys.* **2** (1998) 253 [[hep-th/9802150](#)].
- [40] S. Gubser, I. Klebanov and A. Polyakov, *Gauge theory correlators from non-critical string theory*, *Physics Letters B* **428** (1998) 105.
- [41] S.A. Hartnoll, *Lectures on holographic methods for condensed matter physics*, *Classical and Quantum Gravity* **26** (2009) 224002.
- [42] C.P. Herzog, *Lectures on holographic superfluidity and superconductivity*, *Journal of Physics A: Mathematical and Theoretical* **42** (2009) 343001.
- [43] J. McGreevy, *Holographic duality with a view toward many-body physics*, *Advances in High Energy Physics* **2010** (2010) 723105.
- [44] G.T. Horowitz, *Introduction to holographic superconductors*, in *From Gravity to Thermal Gauge Theories: The AdS/CFT Correspondence: The AdS/CFT Correspondence*, E. Papantonopoulos, ed., (Berlin, Heidelberg), pp. 313–347, Springer Berlin Heidelberg (2011), [DOI](#).
- [45] S. Sachdev, *Condensed matter and ads/cft*, in *From Gravity to Thermal Gauge Theories: The AdS/CFT Correspondence: The AdS/CFT Correspondence*, E. Papantonopoulos, ed., (Berlin, Heidelberg), pp. 273–311, Springer Berlin Heidelberg (2011), [DOI](#).
- [46] S. Kachru, A. Karch and S. Yaida, *Holographic lattices, dimers, and glasses*, *Phys. Rev. D* **81** (2010) 026007.
- [47] S. Kachru, A. Karch and S. Yaida, *Adventures in holographic dimer models*, *New Journal of Physics* **13** (2011) 035004.
- [48] W. Mück, *Polyakov loop of antisymmetric representations as a quantum impurity model*, *Phys. Rev. D* **83** (2011) 066006.
- [49] A. Faraggi and L.A. Pando Zayas, *The spectrum of excitations of holographic wilson loops*, *Journal of High Energy Physics* **2011** (2011) 18.
- [50] K. Jensen, S. Kachru, A. Karch, J. Polchinski and E. Silverstein, *Towards a holographic marginal fermi liquid*, *Phys. Rev. D* **84** (2011) 126002.
- [51] N. Karaiskos, K. Sfetsos and E. Tsatis, *Brane embeddings in sphere submanifolds*, *Classical and Quantum Gravity* **29** (2011) 025011.
- [52] S. Harrison, S. Kachru and G. Torroba, *A maximally supersymmetric kondo model*, *Classical and Quantum Gravity* **29** (2012) 194005.
- [53] P. Benincasa and A.V. Ramallo, *Fermionic impurities in chern-simons-matter theories*, *Journal of High Energy Physics* **2012** (2012) 76.
- [54] A. Faraggi, W. Mück and L.A. Pando Zayas, *One-loop effective action of the holographic antisymmetric wilson loop*, *Phys. Rev. D* **85** (2012) 106015.

- [55] P. Benincasa and A.V. Ramallo, *Holographic kondo model in various dimensions*, *Journal of High Energy Physics* **2012** (2012) 133.
- [56] G. Itsios, K. Sfetsos and D. Zoakos, *Fermionic impurities in the unquenched abjm*, *Journal of High Energy Physics* **2013** (2013) 38.
- [57] J. Erdmenger, C. Hoyos, A. O'Bannon and J. Wu, *A holographic model of the kondo effect*, *Journal of High Energy Physics* **2013** (2013) 86.
- [58] A. O'Bannon, I. Papadimitriou and J. Probst, *A holographic two-impurity kondo model*, *Journal of High Energy Physics* **2016** (2016) 103.
- [59] J. Erdmenger, M. Flory, C. Hoyos, M.-N. Newrzella and J.M.S. Wu, *Entanglement entropy in a holographic kondo model*, *Fortschritte der Physik* **64** (2016) 109
[<https://onlinelibrary.wiley.com/doi/pdf/10.1002/prop.201500099>].
- [60] J. Erdmenger, M. Flory, C. Hoyos, M.-N. Newrzella, A. O'Bannon and J.M.S. Wu, *Holographic impurities and kondo effect*, *Fortschritte der Physik* **64** (2016) 322
[<https://onlinelibrary.wiley.com/doi/pdf/10.1002/prop.201500079>].
- [61] J. Erdmenger, C. Hoyos, A. O'Bannon, I. Papadimitriou, J. Probst and J.M.S. Wu, *Two-point functions in a holographic kondo model*, *Journal of High Energy Physics* **2017** (2017) 39.
- [62] J. Erdmenger, M. Flory, M.-N. Newrzella, M. Strydom and J.M.S. Wu, *Quantum quenches in a holographic kondo model*, *Journal of High Energy Physics* **2017** (2017) 45.
- [63] J. Erdmenger, C. Hoyos, A. O'Bannon, I. Papadimitriou, J. Probst and J.M.S. Wu, *Holographic kondo and fano resonances*, *Phys. Rev. D* **96** (2017) 021901.
- [64] B. Padhi, A. Tiwari, C. Setty and P.W. Phillips, *Log-rise of the resistivity in the holographic kondo model*, *Phys. Rev. D* **97** (2018) 066012.
- [65] J. Erdmenger, C.M. Melby-Thompson and C. Northe, *Holographic rg flows for kondo-like impurities*, *Journal of High Energy Physics* **2020** (2020) 75.
- [66] S. Sachdev, *Holographic metals and the fractionalized fermi liquid*, *Phys. Rev. Lett.* **105** (2010) 151602.
- [67] S. Sachdev, *Strange metals and the ads/cft correspondence*, *Journal of Statistical Mechanics: Theory and Experiment* **2010** (2010) P11022.
- [68] E. Oh, Y. Seo, T. Yuk and S.-J. Sin, *Ginzberg-landau-wilson theory for flat band, fermi-arc and surface states of strongly correlated systems*, *Journal of High Energy Physics* **2021** (2021) 53.
- [69] S. Sukrakarn, T. Yuk and S.-J. Sin, *Mean field theory for strongly coupled systems: Holographic approach*, *JHEP* **06** (2024) 100 [[2311.01897](https://arxiv.org/abs/2311.01897)].
- [70] J.N. Laia and D. Tong, *A holographic flat band*, *Journal of High Energy Physics* **2011** (2011) 125.
- [71] Y.-K. Han, J.-W. Seo, T. Yuk and S.-J. Sin, *Holographic lieb lattice and gapping its dirac band*, *Journal of High Energy Physics* **2023** (2023) 84.
- [72] M. Čubrović, J. Zaanen and K. Schalm, *String theory, quantum phase transitions, and the emergent fermi liquid*, *Science* **325** (2009) 439
[<https://www.science.org/doi/pdf/10.1126/science.1174962>].

- [73] S.-S. Lee, *Non-fermi liquid from a charged black hole: A critical fermi ball*, *Phys. Rev. D* **79** (2009) 086006.
- [74] N. Iqbal and H. Liu, *Real-time response in ads/cft with application to spinors*, *Fortschritte der Physik* **57** (2009) 367
[<https://onlinelibrary.wiley.com/doi/pdf/10.1002/prop.200900057>].
- [75] H. Liu, J. McGreevy and D. Vegh, *Non-fermi liquids from holography*, *Phys. Rev. D* **83** (2011) 065029.
- [76] T. Faulkner, N. Iqbal, H. Liu, J. McGreevy and D. Vegh, *Holographic non-fermi-liquid fixed points*, *Philosophical Transactions of the Royal Society A: Mathematical, Physical and Engineering Sciences* **369** (2011) 1640
[<https://royalsocietypublishing.org/doi/pdf/10.1098/rsta.2010.0354>].
- [77] Y. Liu and Y.-W. Sun, *Topological nodal line semimetals in holography*, *Journal of High Energy Physics* **2018** (2018) 72.
- [78] Y. Seo, G. Song, Y.-H. Qi and S.-J. Sin, *Mott transition with holographic spectral function*, *Journal of High Energy Physics* **2018** (2018) 77.
- [79] S. Chakrabarti, D. Maity and W. Wahlang, *Probing the holographic fermi arc with scalar field: numerical and analytical study*, *Journal of High Energy Physics* **2019** (2019) 37.
- [80] E. Oh, T. Yuk and S.-J. Sin, *The emergence of strange metal and topological liquid near quantum critical point in a solvable model*, *Journal of High Energy Physics* **2021** (2021) 207.
- [81] T. Yuk and S.-J. Sin, *Flow equation and fermion gap in the holographic superconductors*, *Journal of High Energy Physics* **2023** (2023) 121.
- [82] J.I. Kapusta and C. Gale, *Finite-Temperature Field Theory: Principles and Applications*, Cambridge Monographs on Mathematical Physics, Cambridge University Press, 2 ed. (2006).
- [83] W.-J. Li and H. Zhang, *Holographic non-relativistic fermionic fixed point and bulk dipole coupling*, *Journal of High Energy Physics* **2011** (2011) 18.
- [84] J.-W. Rhim and B.-J. Yang, *Singular flat bands*, *Advances in Physics: X* **6** (2021) 1901606.
- [85] M. Nakahara, *Geometry, topology and physics*, CRC Press (2003).
- [86] A. Altland and B.D. Simons, *Condensed Matter Field Theory*, Cambridge University Press, 2 ed. (2010), [10.1017/CBO9780511789984](https://doi.org/10.1017/CBO9780511789984).
- [87] M. Vojta, *Quantum phase transitions*, *Reports on Progress in Physics* **66** (2003) 2069.